Theses and Dissertations

2017

Cable Health Monitoring System Built Into Power Converter Using Time Domain Reflectometry

Hossein Baninajar
University of South Carolina

Follow this and additional works at: http://scholarcommons.sc.edu/etd

Part of the Electrical and Electronics Commons

CABLE HEALTH MONITORING SYSTEM BUILT INTO POWER CONVERTER USING
TIME DOMAIN REFLECTOMETRY

by

Hossein Baninajar

Bachelor of Science
Chamran University of Ahvaz, 2007

_____

Submitted in Partial Fulfillment of the Requirements

For the Degree of Master of Science in

Electrical Engineering

College of Engineering and Computing

University of South Carolina

2017

Accepted by:

Enrico Santi, Director of Thesis

Andrea Benigni, Reader

Cheryl L. Addy, Vice Provost and Dean of the Graduate School

DEDICATION

To my wife, Neda for all of her love and support and to my mother and my late father who are my teachers for my lifetime.

ACKNOWLEDGEMENTS

ABSTRACT

Aging cables are a critical reliability concern for many electrical systems. Cables run over long distances, are often exposed to harsh environments and are intended to work for several decades. Cable faults can be a serious problem because cables are usually hard to repair or replace. Condition based maintenance is a popular approach that provides high reliability and low maintenance cost at the same time. This is a non-destructive method that collects information about the health condition of the cable under test without causing any potential damage.

Nowadays, in several applications power cables are connected to power converters and it would be desirable to be able to implement condition based maintenance by using the existing converter for cable health monitoring during normal system operation. In this thesis, we investigate the feasibility of using existing power converters to perform online cable health monitoring and propose an add-on circuit which can be added to an existing power converter so that it can perform the health monitoring function. We use the time domain reflectometry method to characterize and locate faults in the cable connecting the output of a power converter to its load.

TABLE OF CONTENTS

LIST OF ABBREVIATIONS

AWG .... American Wire Gauge

DC .... Direct Current

FDR .... Frequency Domain Reflectometry

GaN .... Gallium Nitride

IGBT .... Insulated-Gate Bipolar Transistor

JTFDR .... Joint Time-Frequency Domain Reflectometry

LSB .... Least Significant bit

STDR .... Spectral Time-Domain Reflectometry

CHAPTER 1

INTRODUCTION

Nowadays, systems designed to manage equipment maintenance are considered analogous to health care systems intended to manage human health. A maintenance engineer, just like a physician, monitors the equipment condition and performs any procedure required to ensure that the system runs without problems. There are various factors that define the importance of certain equipment for system operation. For example, a certain piece of equipment may have the largest role in production; another one may have the highest risk of failure. Some equipment, in spite of its high reliability, may cause a long downtime in case of failure, and therefore requires special reliability considerations.

There are different departments in every plant such as production, maintenance, R&D and energy departments. To get the best result, these departments must integrate. In this case, maybe certain equipment is not important from production or maintenance points of view, but because of energy or environmental concerns, its maintenance has the highest priority. A maintenance plan can be developed based on different approaches. The first approach can be called the corrective approach, or the run-to-failure approach. It satisfied the early industrial needs. As industries developed, the preventive approach was introduced which was based on overhaul or replacement of a part or the entire device after a specified time interval related to the mean time to failure. This plan may reduce the frequency of emergency breakdowns, however it has drawbacks, because a failure

may happen either sooner or later than the scheduled replacement time. In the first case the emergency breakdown is not prevented with associated downtime costs. In the second case, incurred replacement costs are larger than necessary. To cope with this issue, the predictive approach was proposed. It is based on some kind of continuous monitoring of the equipment condition. In this method, not only the current condition but also the trend change of condition and the baseline are considered to evaluate the equipment health. To implement this method, several maintenance devices are required which measure different parameters for different types of equipment [1].

Cables are important parts of electrical systems. Since they often are less accessible, in case of failure it takes more time and cost to get them fixed. Moreover, unlike other electrical equipment which is installed in clean, sealed and air-conditioned rooms, they frequently are deployed in harsh condition, and during operation are exposed to mechanical and thermal stress, corrosion, water and even radiation. As mentioned earlier, they are often inaccessible, and since in some cases they are buried underground or placed inside a tight tunnel, this makes visual inspection impossible. This is the reason why cable condition based monitoring is so important.

Modern loads require controllable voltage and current to work well and efficiently. To satisfy this requirement the use power converters is increasing. Frequently the power is transferred to the loads through power converters and cables.

In this thesis, we are going to introduce a method which uses time domain reflectometry, and can be applied to an existing power converter to give it the ability to perform online cable health monitoring.

This thesis is organized as follows: in Chapter 2, we describe the most important reflectometry methods which have been used for cable fault detection. In Chapter 3, we focus on time domain reflectometry and explain its principles of operation. In Chapter 4, we introduce the proposed method to implement the time domain reflectometry using an existing power converter, then in Chapter 5, we demonstrate the feasibility of the method by discussing the experimental result and finally in Chapter 6 we summarize the work and make suggestions for future work.

CHAPTER 2

A BRIEF REVIEW OF REFLECTOMETRY METHODS

2.1 ABSTRACT

Cables like veins in the human body distribute the power throughout the electrical system. Indeed, they are the backbone of the transmission and distribution systems. The more important a part is, the more monitoring is required to make sure it is in the safe zone of operation. There are different types of cable fault detection methods. They can be categorized into several classes; online and offline, destructive and non-destructive and so on. Addressing all methods is outside the scope of this thesis. In this Chapter, we are going to focus on describing and comparing several reflectometry methods such as Time Domain Reflectometry (TDR), Frequency Domain Reflectometry (FDR), Spectral Time-Domain Reflectometry (STDR) and Joint Time-Frequency Domain Reflectometry (JTFDR).

2.2 INTRODUCTION

The reflectometry method is often said to be a radar method because it is based on sending a signal to a transmission line and analyzing the reflected signal [2]. The sending signal, called incident waveform, has a reflection once it encounters a discontinuity. Discontinuity could be any deviation from the normal condition of the cable. Different reflectometry methods use different incident waveforms: time domain reflectometry uses

a fast step stimulus waveform; frequency domain reflectometry uses a swept frequency signal; sequence TDR uses pseudo noise: and joint time-frequency domain reflectometry uses a linearly modulated chirp signal with a Gaussian envelope.

2.3 TIME DOMAIN REFLECTOMETRY

Time domain reflectometry (TDR) uses an incident waveform with a fast rise time. A simple TDR setup consists of a step generator producing the incident waveform, which typically is a square wave, and sending it into the line. The incident waveform travels through the line with a propagation velocity related to cable physical characteristics and has a reflection if it encounters any impedance discontinuity. The reflection coefficient is defined as the ratio of reflected wave to incident wave and it can be seen as an index of discontinuity impedance. The location of the discontinuity can be determined if the round-trip delay and propagation velocity are known [3].

Since the TDR method is the main method we are going to apply in our proposed system, we describe it here briefly, and we will describe it in detail in the next Chapter.

2.4 SPECTRAL TIME DOMAIN REFLECTOMETRY

Spectral time domain reflectometry (STDR) uses a low-amplitude pseudo noise (PN) signal as incident wave. The signal amplitude is very small. It needs to be large enough to ensure a good signal-to-noise ratio, but it can be much smaller than other system signals. Therefore, it enables the online monitoring of the cable without interfering with the normal operation of the system. Location and type of the fault can be determined from the correlation between the incident and reflected wave [4]. In [5] a

CMOS sensor which is a novel architecture was developed to implement the STDR method on a 0.5- μm integrated circuit. The sensor locates short or open circuits on active wires with an accuracy of +/-1 ft when running at a clock speed of 100 MHz. Shown in Fig. 2.1 is the spectral time domain reflectometry structure.
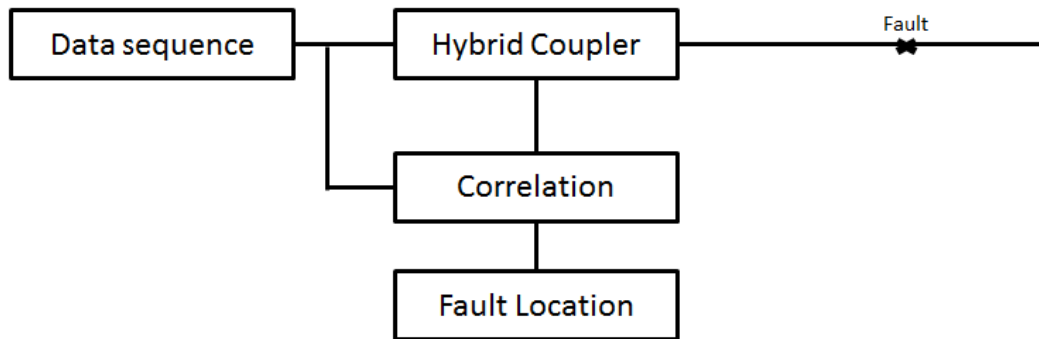

Fig. 2.1 Spectral time domain reflectometry structure

2.5 FREQUENCY DOMAIN REFLECTOMETRY

As mentioned before, all reflectometry methods share the same principle of operation. In the frequency domain reflectometry (FDR) method, a linearly swept frequency signal is used as incident wave. A linearly swept frequency signal is a sinusoidal signal with frequency that increases linearly with time. The incident wave is transmitted into the line and has a reflection after it sees any discontinuity. After a time equal to the round-trip time, the reflected wave arrives at the transmitting point. At that time the incident generator is injecting a new sine wave with a higher frequency, as it is expected based on the definition of swept frequency signal above. Similar to TDR, where round trip time is used to find the discontinuity location, in FDR, the round-trip time can be calculated using the frequency difference between the incident and the reflected wave,

6

knowing that the frequency increases linearly versus time [4]. The Fig. 2.2 shows the frequency domain reflectometry structure.
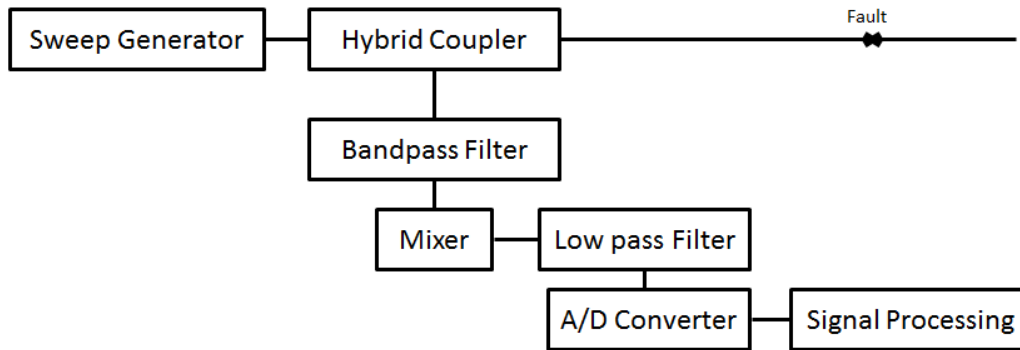

Fig. 2.2 Frequency domain reflectometry structure

Note that the propagation velocity is the key factor for locating the fault. Since we are working in the frequency domain, it is easy to compensate for variable propagation velocity with frequency. This holds true also for attenuation, which also varies with frequency.

With FDR, it is possible to locate different faults at the same time on a cable. Each fault produces a specific reflected wave which has a specific frequency. By using Fourier transform, all the frequency components can be measured. Each component corresponds to a specific fault at a specific distance along the cable. The distance can be calculated from the frequency value.

2.6 JOINT TIME-FREQUENCY DOMAIN REFLECTOMETRY

So far, the time domain and frequency domain reflectometry methods have been described. Joint Time-Frequency Domain Reflectometry (JTFDR) operates in both time and frequency domains because of the type of incident wave used. In JTFDR, the incident wave is a linearly modulated chirp signal with a Gaussian envelope which is defined in time and frequency domains jointly:

$$s(t) = \left(\frac{\alpha}{\pi}\right)^{\frac{1}{4}} e^{-\frac{\alpha(t-t_0)^2}{2} + \frac{j\beta(t-t_0)^2}{2} + j\omega_0(t-t_0)} \tag{2-1}$$

where α, β, t_0 and ω_0 determine the time duration, frequency sweep rate, time center and frequency center, respectively. To have the best results, these parameters can be customized for each specific case based on the cable type and length and available instruments. JTFDR takes advantages of both time and frequency characteristic of its incident wave [6]. Shown in Fig. 2.3 is the diagram that describes the configuration and function of the experimental devices of the JTFDR. A computer (PC) instructs the arbitrary waveform generator to produce the Gaussian-chirp incident signal. This incident signal propagates into the cable under test, is reflected at the fault location, and travels back to the source. A circulator is used as the signal launcher/receiver. The reflected signal is redirected to the digital oscilloscope [7].
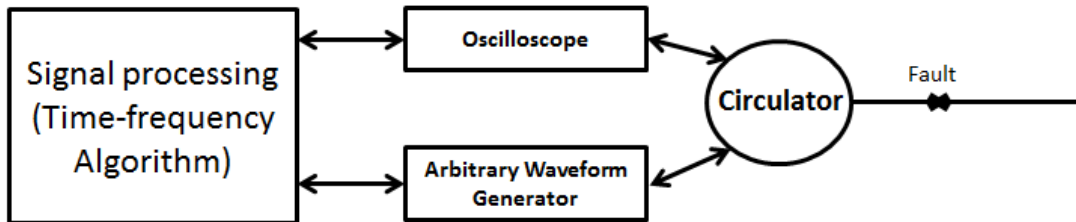

Fig. 2.3 Time-frequency domain reflectometry structure [8]

To detect and locate the fault, the cross correlation of the time-frequency distribution of the incident and reflected waves needs to be calculated.

CHAPTER 3

PRINCIPLES OF TIME DOMAIN REFLECTOMETRY

3.1 INTRODUCION

As mentioned before, the reflectometry method is often said to be a radar method because it is based on sending a signal into a transmission line and analyzing the reflected signal. To understand in detail how time domain reflectometry works, an effective understanding of transmission lines is needed beforehand.

3.2 TRANSMISSION LINE

A transmission line is used to transfer electrical power from a generation or distribution side to a consumption side or load. Based on the surrounding environment, voltage and current rating and other application criteria, different types of transmission line may be used for different applications.

The simplest transmission line in electrical power system consists of two conductors. It can be a coaxial cable, twisted pair cable and so on. If we consider the transmission line as a system, we can find a model which describes it based on certain electrical parameters. These parameters are resistance, conductance, capacitance, and inductance. We expect a transmission line to be lossless or at least low loss because, if it is not, it cannot be considered for the purpose of transferring power. So, in most cases, the line losses are neglected, which means that resistance and conductance can be neglected in transmission line modelling.

As mentioned before, the transmission line consists of two conductors with some dielectric insulator between them. Notice that this is the definition of a capacitor. The time-varying current flowing in a conductor produces a time-varying magnetic field, which induces an electric and magnetic field in the conductors. Therefore, there is flux linkage between the two conductors. The inductance is the ratio of this flux linkage divided by the conductor current.

A lossless transmission line is practically impossible to realize. However, if R≪ωL and G≪ωC, ignoring resistance and conductance still gives a good approximation. So, the transmission line can be modeled by only L and C. A balanced transmission line (two wire cable) is shown in Fig. 3.1.A while Fig. 3.1.B shows the model for a coaxial cable which is an unbalanced line.
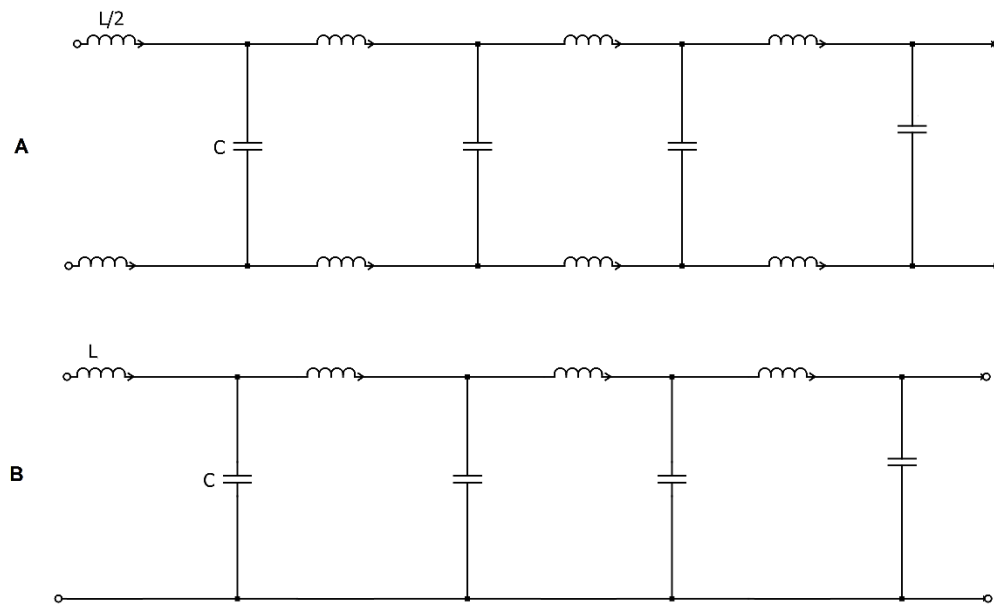

Fig. 3.1 Transmission line model. A) balanced, B) unbalanced

Characteristic impedance is defined as the ratio of the amplitude of voltage and current propagating through the line. The characteristic impedance, Z_0 in ohm is:

$$Z_0 = \sqrt{\frac{L}{C}} \tag{3-1}$$

The characteristic impedance can also be calculated using the geometry parameters of the coaxial cable,

$$Z_0 = \frac{138.2}{\sqrt{\epsilon_r}} \log_{10} \frac{D}{d} \tag{3-2}$$

where ε_r is dielectric constant and D and d are the dielectric and central conductor diameters, respectively. In this formula, the dielectric material is assumed to be non-magnetic and therefore the relative permeability is unity. As these formulas obviously show, the characteristic impedance is constant unless the line characteristics change. The change can be any increase or decrease in wire size or distance between them (or a change in dielectric constant). In a matched transmission line, any change in characteristic impedance causes a reflection.

Propagation velocity is another important parameter. It is related to the time it takes for an electromagnetic wave to propagate through a transmission line. The propagation velocity in free space is given by the speed of light $v_C = 3 \times 10^8 m/s$. The propagation velocity of a wave in a coaxial cable is:

$$v_P = \frac{1}{\sqrt{L \cdot C}} \tag{3-3}$$

In this formula, L and C are per unit length values.

The dielectric material between two conductors determines the velocity of propagation in a transmission line. Using above formula, propagation velocity in free space and propagation velocity in the dielectric material are related by this this formula:

$$v_P = \frac{v_c}{\sqrt{\varepsilon_r}} \qquad\qquad (3\text{-}4)$$

As a matter of fact, the lossless transmission line is impossible in practice, so in reality there is always power loss, which causes attenuation. Attenuation is defined in terms of decibels per unit length or nepers per unit length at a given frequency and consists of resistive loss and dielectric loss. Attenuation is frequency dependent, and their relation is nonlinear [9].

3.3 TIME DOMAIN REFLECTOMETRY

The time domain reflectometry setup consists of a step generator producing the incident waveform, which typically is a square wave, and sending it into the line. The incident waveform travels through the line with propagation velocity v_p and a reflection occurs if it encounters any impedance discontinuity. A high-speed oscilloscope displays both incident and reflected waveform. A simple diagram of a time domain reflectometry setup is shown in Fig. 3.2 [10].
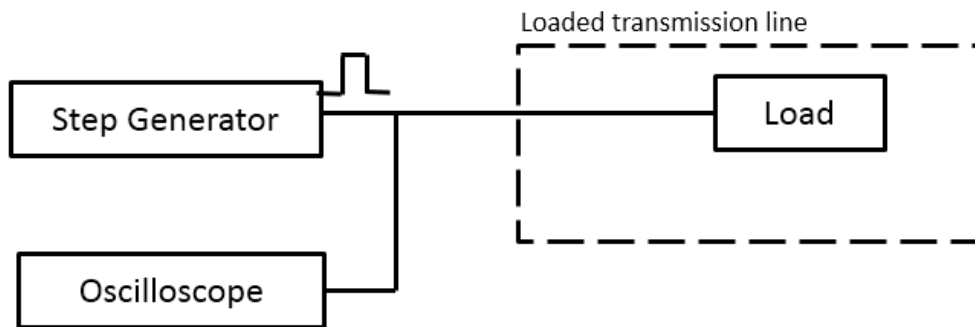
Fig. 3.2 Block diagram of a simple time domain reflectometry setup

Due to the finite propagation velocity, there is a time delay between the incident and reflected waveform. This time delay is the time needed for the wave to return to the

source after seeing a discontinuity. The location of the mismatch can be determined by knowing this round-trip delay and propagation velocity. The distance D between the discontinuity and the step generating point is

$$D = v_P \cdot \frac{T}{2} \tag{3-5}$$

where T is the round-trip delay.

If the incident wave encounters a discontinuity, a reflected and a transmitted waveforms are generated. The transmitted waveform continues in the forward direction and the reflected waveform goes back to the source. To derive a formula for reflection coefficient in a transmission line, let us assume a lossless transmission line with characteristic impedance Z_0 terminated in a load impedance Z_L which depicted in Fig. 3.3 [11].
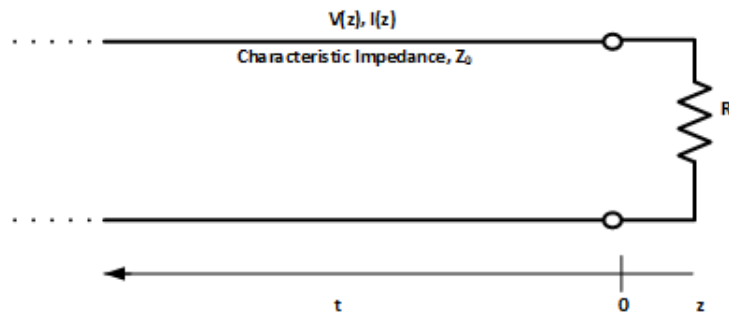
Fig. 3.3 An unmatched transmission line

Suppose an incident waveform of the form $V_0^+ e^{-j\beta z}$ is generated at generating point and travelling toward the load which β is the propagation constant and is defined as $\beta \approx \omega \sqrt{(L.C)}$. By definition of characteristic impedance, the ratio of voltage to current is

14

Z_0. However, at the load, this ratio must be Z_L. To satisfy this equation, a reflected waveform must be excited. The total voltage and current on the line are given by

$$V(z) = V_0^+ e^{-j\beta z} + V_0^- e^{j\beta z} \qquad (3\text{-}6)$$

$$I(z) = \frac{V_0^+}{Z_0} e^{-j\beta z} - \frac{V_0^-}{Z_0} e^{j\beta z} \qquad (3\text{-}7)$$

where V_0^- is the amplitude of the reflected waveform.

The ratio of voltage to current at the load (z=0) is

$$Z_L = \frac{V(0)}{I(0)} = \frac{V_0^+ + V_0^-}{V_0^+ - V_0^-} Z_0 \qquad (3\text{-}8)$$

Solving for V_0^- gives

$$V_0^- = \frac{Z_L - Z_0}{Z_L + Z_0} V_0^+ \qquad (3\text{-}9)$$

The reflection coefficient is the ratio of the amplitude of the reflected wave to the incident wave, i.e.,

$$\Gamma = \frac{V_0^-}{V_0^+} = \frac{Z_L - Z_0}{Z_L + Z_0} \qquad (3\text{-}10)$$

In theory, knowing the reflection coefficient and the line impedance it is possible to calculate load impedance Z_L, which represents the fault. As mentioned, the lossless transmission line is impossible in practice. So, the pulses get distorted as they travel through the line, and it can be difficult to classify faults just by calculating the value of the reflection coefficient. On the other hand, notice that locating the fault is relatively easy.

Though we always consider impedance Z_0 as a real number (lossless line), load impedance or, in other words, discontinuity impedance could be a complex number. Magnitude, sign, and the shape of the reflected signal, define the nature of the fault. All of this information is summarized in the reflection coefficient [10].

3.4. BEHAVIOR OF DIFFERENT FAULTS

To give a better understanding of how the fault characteristic can be recognized by knowing the reflection coefficient, the Fig. 3.4 illustrates typical fault types. In all cases, the fault impedance is assumed to be a real number. Since the characteristic impedance of the line is also a real number for a losslessline, the reflection coefficient is a real number as well.
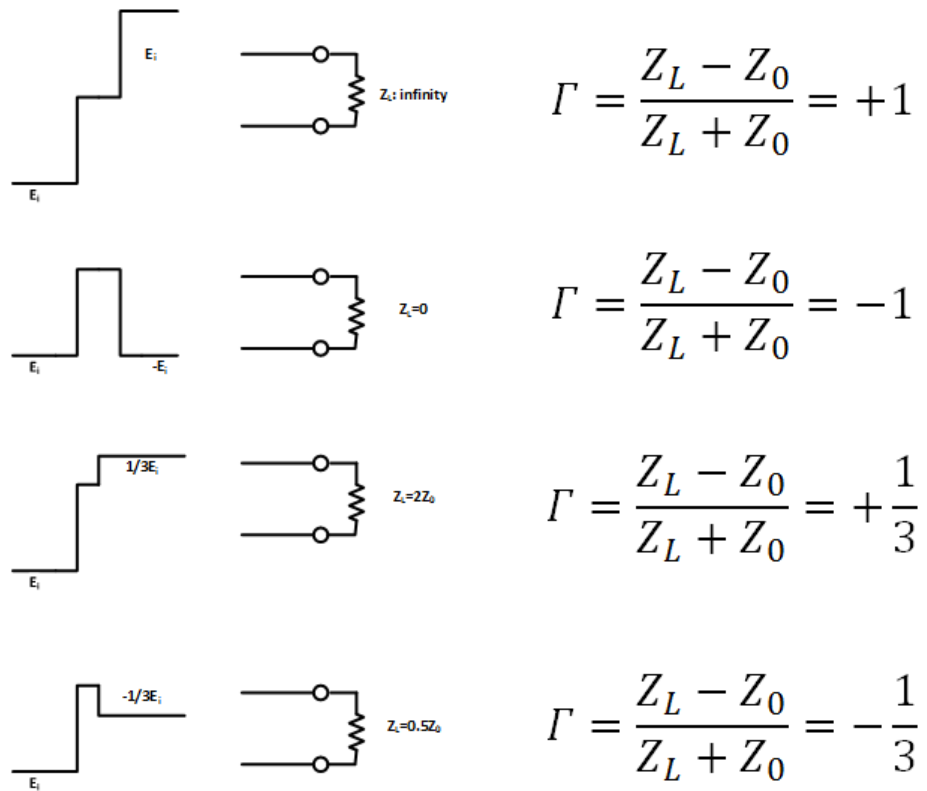
$$\Gamma = \frac{Z_L - Z_0}{Z_L + Z_0} = +1$$

$$\Gamma = \frac{Z_L - Z_0}{Z_L + Z_0} = -1$$

$$\Gamma = \frac{Z_L - Z_0}{Z_L + Z_0} = +\frac{1}{3}$$

$$\Gamma = \frac{Z_L - Z_0}{Z_L + Z_0} = -\frac{1}{3}$$

Fig. 3.4 Reflection coefficient for different discontinuities

In Fig. 3.5 we consider some more realistic cases. In reality, the fault impedance is a complex number. In the following cases, the fault is modeled as the combination of Rs, Ls, and Cs. Two approaches can be taken to find out the behavior of the reflected signal regarding the fault: a mathematical approach and a simplified approach based on the frequency domain characteristics of impedances.

16

Following the mathematical approach, the reflection coefficient and the incident signal are calculated in the Laplace domain and the reflected signal is obtained by multiplying them together. Now, to find an expression for the reflected signal, the Laplace inverse transformation of the calculated reflected signal must be taken. This approach is rather mathematical and abstract.
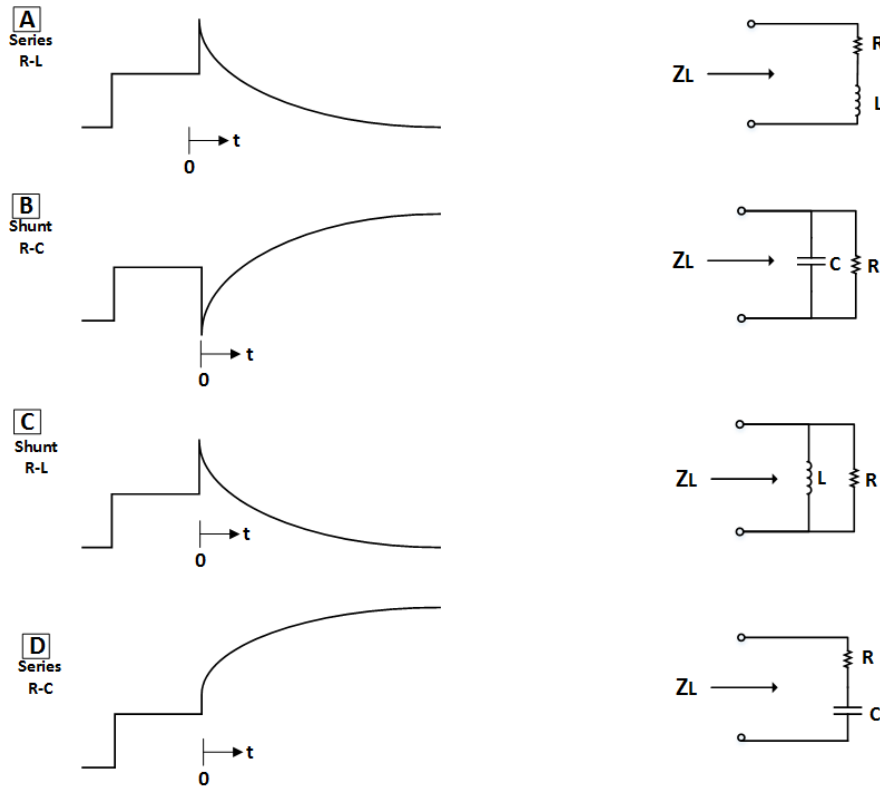

Fig. 3.5 TDR with non-real discontinuity impedance

The second approach is somehow more intuitive. It utilizes the frequency-dependent behavior of capacitors and inductors. Let us consider the case of a capacitive discontinuity. The capacitive reactance is inversely proportional to frequency. This means that at higher frequency its reactance goes to zero and at low frequency it goes to infinity. If it is translated in the time domain for the case of a step response, the capacitor behaves as a short circuit at t=0 (high frequency signal components) and behaves as an open

circuit at t = ∞ (zero frequency). The reflected waveform behaves exponentially between t=0 and t = ∞. The inductor behavior is also frequency-dependent similar to a capacitor, with the only difference that an inductor behaves as an open circuit at t=0 and as a short circuit at t = ∞.

The intuitive approach gives the ability to simply analyze the behavior of reflected signal in response to a discontinuity and reciprocally to interpret the nature of a discontinuity just by observing the reflected signal characteristics [10].

3.5 INTERMEDIATE DISCONTINUITY

So far we have studied different mismatched terminations. However, the discontinuity can occur anywhere along the cable. The harsh environment affects the cable more in the region far away from the two ends of the cable, so having a fault in these regions is more frequent. Dealing with a discontinuity at an intermediate position along the cable is not different from analyzing a mismatched termination. The Fig. 3.6 shows an intermediate discontinuity which is a change in characteristic impedance of the cable and Fig. 3.7 demonstrates the TDR trace for a special case which is an inductive discontinuity.
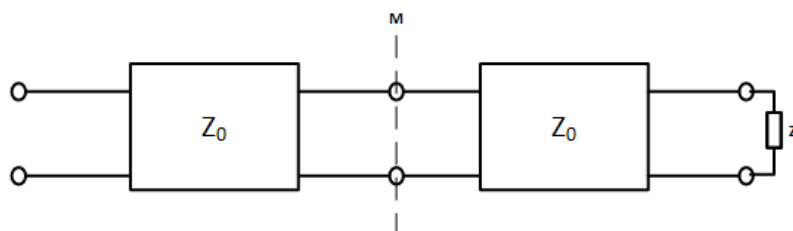
Fig. 3.6 Intermediate discontinuity
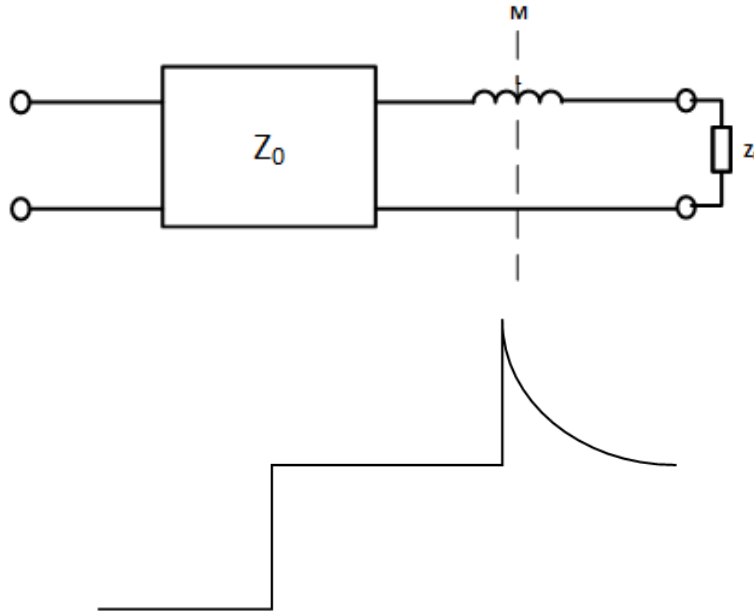
Fig. 3.7 Non-real intermediate discontinuity impedance

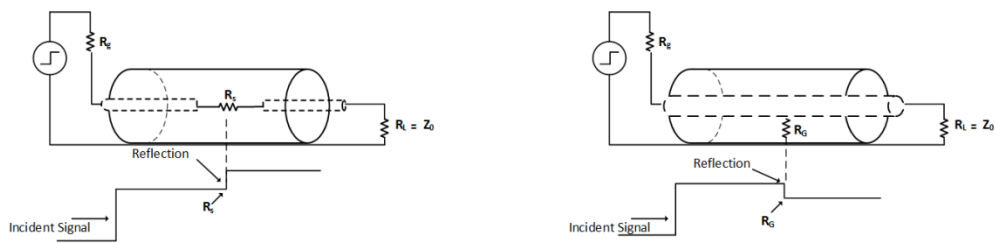In the Fig. 3.8, two resistive intermediate discontinuities with their corrsponding TDR traces have been shown [9].

Fig. 3.8 Single-resistor discontinuity and reflection

A)single series resistor B)single shunt resistor

3.6 MULTIPLE DISCONTINUITIES

The time domain reflectometry method is not only capable of detecting a single discontinuity located at the end or along the cable but also can detect multiple discontinuities along the cable. Assuming the faults are located at different positions as it depicted in Fig. 3.9, it takes a different time for the reflected signal to get back to the source, so the reflected signals are separated in time and can be individually measured as it has been shown in Fig. 3.10 [9].
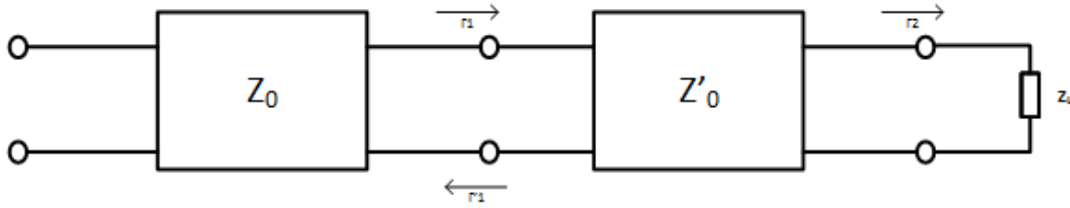
$$Z_0 \neq Z_0' \neq Z_L$$

$$\Gamma_1 = \frac{Z_0' - Z_0}{Z_0' + Z_0} = -\Gamma_1' \qquad \Gamma_2 = \frac{Z_L - Z_0'}{Z_L + Z_0'}$$

Fig. 3.9 Cable with multiple discontinuities
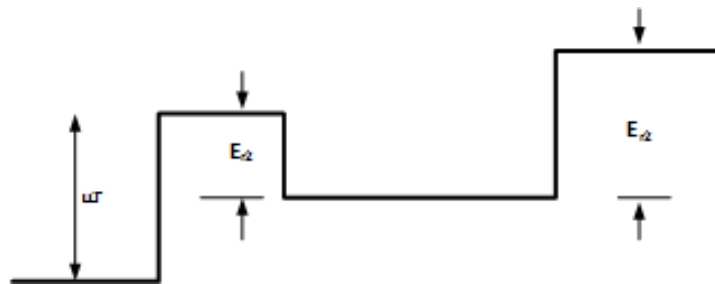
Fig. 3.10 TDR representation of multiple discontinuities

3.7 TIME AND AMPLITUDE RESOLUTION

Resolution refers to the ability of a TDR system to detect and locate very small and closely spaced discontinuities. Amplitude resolution refers to the ability of the TDR system to detect a very small reflected signal which is caused by a very small discontinuity. Time resolution refers to the ability of the TDR system to locate and distinguish two separate discontinuities which are closely located.

Time and amplitude resolution impose limitations on fault detection. If a TDR system does not have sufficient resolution, small or closely-spaced discontinuities cannot be detected and located accurately. Time resolution is limited by incident signal rise time and amplitude resolution is limited by aberration and noise.

Rise time: in order to have a TDR system with a good spatial resolution, the incident wave needs to have a fast rise time. The rising time of the reflected signal at least is equal to the rising time of the incident signal. There are several factors which can make it even longer. So, in the best condition, the time resolution is the half of the system rising time which relates to incident signal rising time.

Aberration: aberration means any departure from what is expected from incident signal. Aberrations have an effect on spatial resolution. Aberrations can occur before or after the main incident signal and will cause some other reflections which can reduce resolution.

Noise: in order to have a TDR system with a good amplitude resolution, the measurement noise should be smaller than the reflected signal amplitude caused by the discontinuity that we are trying to detect. So displayed noise is a good reference to compare different TDR systems regarding amplitude resolution [9], [10].

3.8 TDR CONFIGURATION

From the prior discussion, the goal in every TDR system should be to decrease rise time and measurement noise at the same time. Sometimes this is not possible. In some cases, increasing rise time causes an increase in noise. It all depends on the configuration we choose to implement the TDR system. Fig. 3.11 shows the four different possible configurations for a TDR system [9].
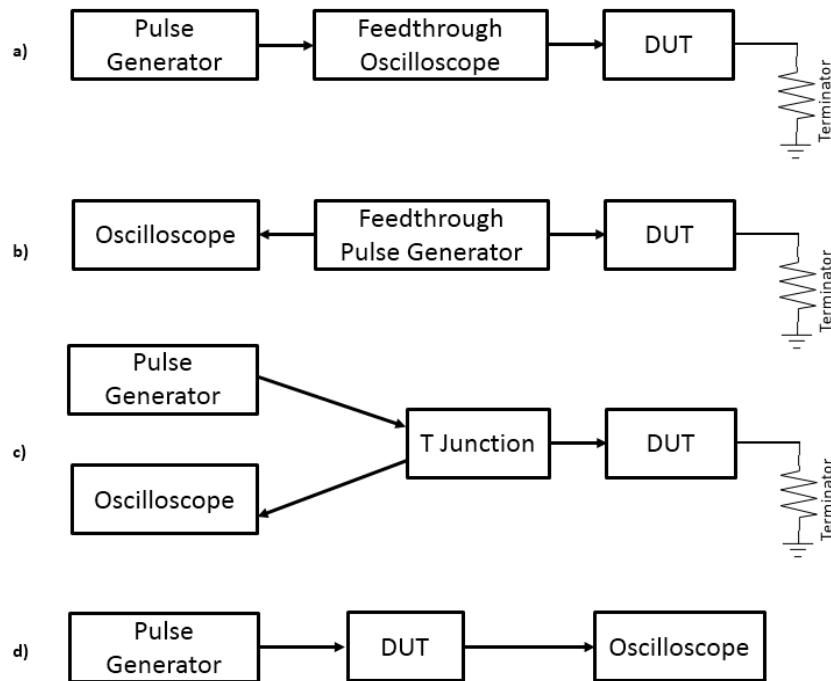

Fig. 3.11 TDR system configuration

Sometimes there are other constraints. In some cases, the situation dictates the measurement and injection points. For example, in some applications, one cable end may be inaccessible, so the injection and measurement must be taken at other side and we may lose some degrees of freedom in selecting the desired configuration.

CHAPTER 4

BUILT-IN TDR FOR POWER CONVERTER

4.1. INTRODUCTION

Nowadays, in several applications, power converters are connected to power cables, so it would very desirable to use power converters to monitor the condition of cables to which they are connected. The objective of this thesis is to investigate how to enable an existing power converter to operate as a TDR system.

In order to achieve this goal, the main parts of a TDR system need to get implemented. Note that the main function of a DC-DC power converter is transferring a pure DC power to the load, so our method should not interfere with this power processing function.

4.2 POWER CONVERTER STRUCTURE

An infinite number of converter structures are possible [12]. Here, we only introduce a simple buck converter which consists of a half bridge circuit and an LC filter.
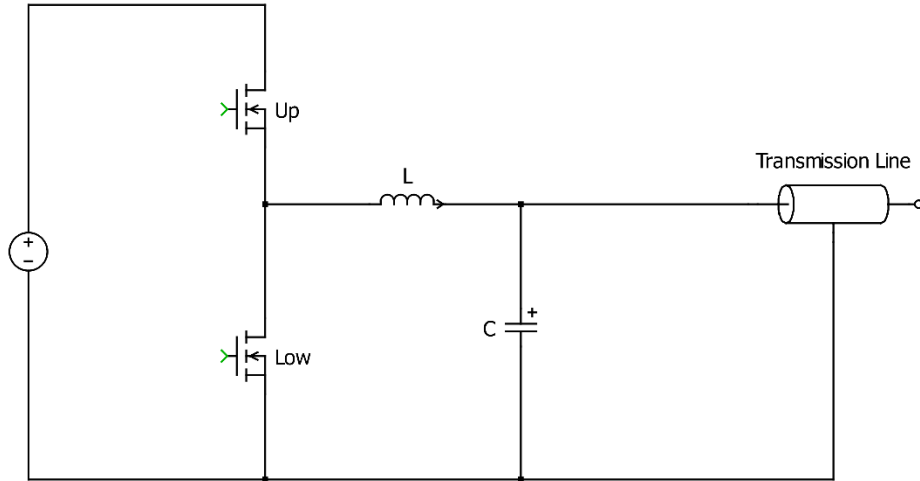
Fig. 4.1 A simple buck converter structure

The input of the half bridge circuit is a DC voltage, and the converter output is DC as well. The upper and lower switches turn on and off in a complementary fashion. The lower switch voltage is shown in Fig. 4.2.
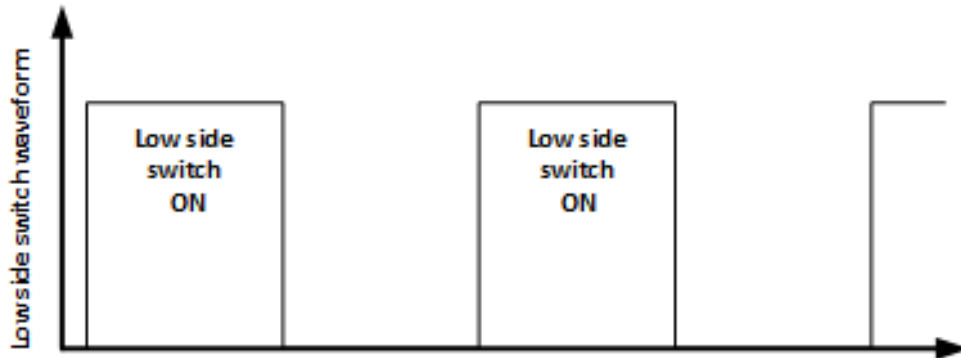

Fig. 4.2 The lower switch voltage waveform

It is a square wave voltage which is the same as a conventional incident signal for a TDR system. However, this signal cannot be directly used for our application, since the L-C low pass filter attenuates the high frequency components applied to the cable. Removing the LC filter is not an option, because it would interfere with the normal operation of the system.

4.3. MODIFICATION TO POWER CONVERTER

The proposed modification is an RC circuit which takes the lower switch voltage as the input and gives a fast rise pulse as the output which can be used as an incident signal for the TDR purposes.
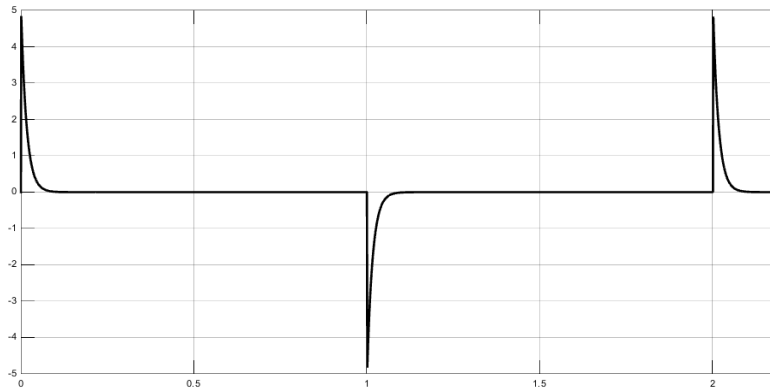
Fig. 4.3 Fast rise signal produced by the RC circuit

The incident wave should be sent to the cable under test. A pulse transformer can properly transfer the incident voltage to the converter output. For proper operation, the pulse transformer should be able to transmit the high-frequency components of the pulse signal. Low transformer leakage inductance is required to make sure that the signal sent along the cable properly tracks the incident signal produced by the injection circuit.
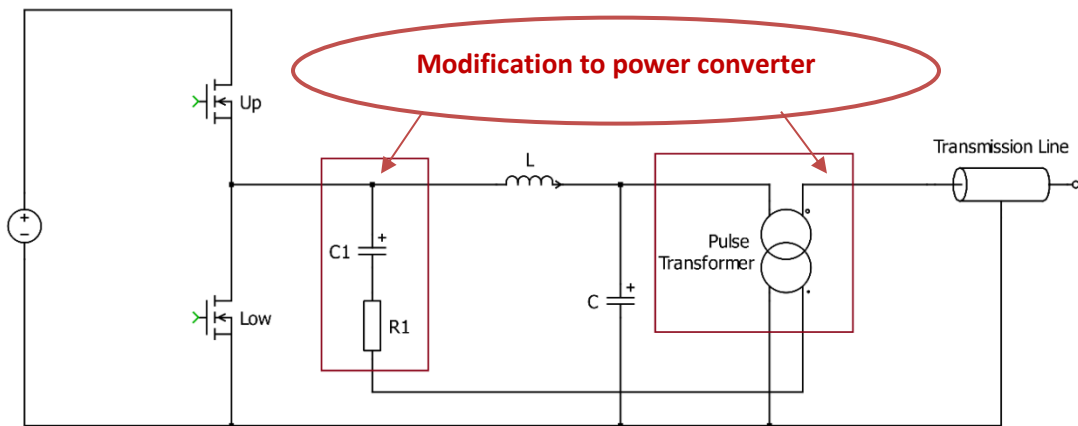
Fig. 4.4 Required modification built into an existing power converter

In the following examples, we show the feasibility of using this incident waveform for TDR purposes. We examine the short circuit and open circuit cases (hard faults) and a soft intermediate fault modeled by a parallel fault. Pspice has a transmission line model which let us simulate different types of discontinuity [13]. The simulation setup is shown in Fig. 5.5.
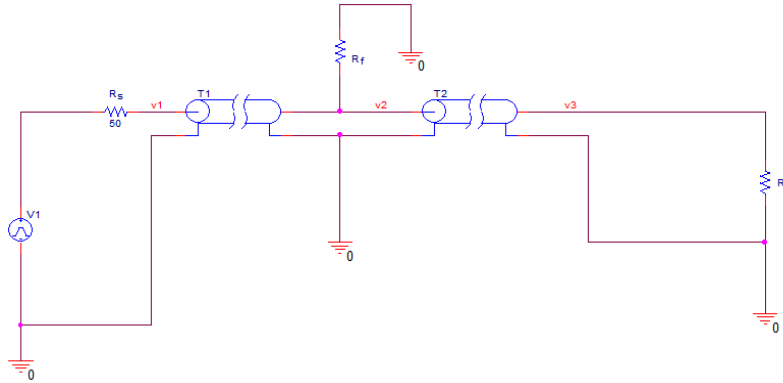

Fig. 4.5 Simulation model for TDR measurement

To simulate the hard faults, two transmission lines, T1 and T2 should be the same and their characteristic impedances should be equal to the source resistance, Rs that is 50Ω. Rf is the parallel fault and is considered as infinity. The load resistance, RL is set 0 and then a large number respectively to simulate the short and open terminations.
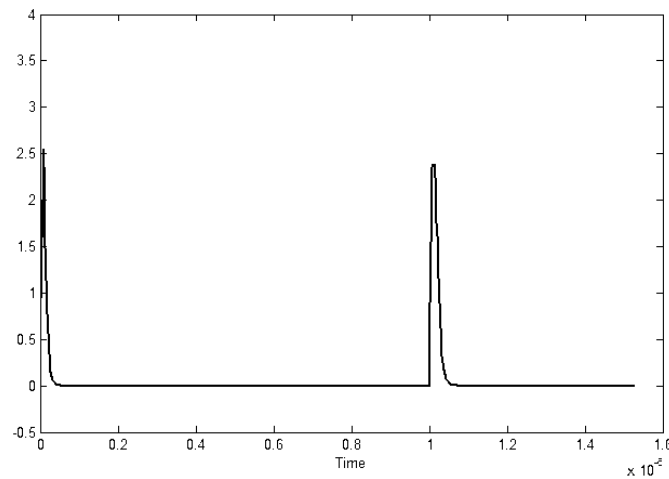

Fig. 4.6 TDR signal for open circuit case (simulation result)
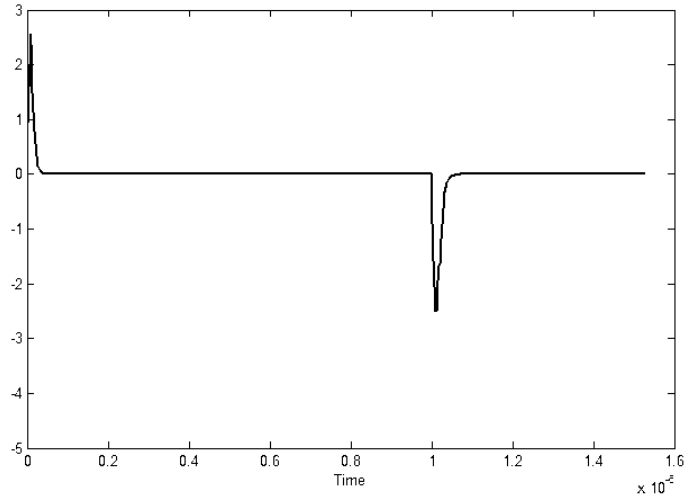
26

Fig. 4.7 TDR signal for short circuit case (simulation result)

As can be seen from the Fig. 4.6 and Fig. 4.7, the reflection coefficients for the open and short circuits are 1 and -1 respectively which are consistent with results using formulas in Chapter 3. The round-trip time is twice the time the incident signal needs to reach the discontinuity.

To simulate the soft fault, the model is the same as before except for the following two changes. First, the load resistance, R_L is equal to 50Ω and second, the parallel load should have a finite value to model the insulation deterioration.
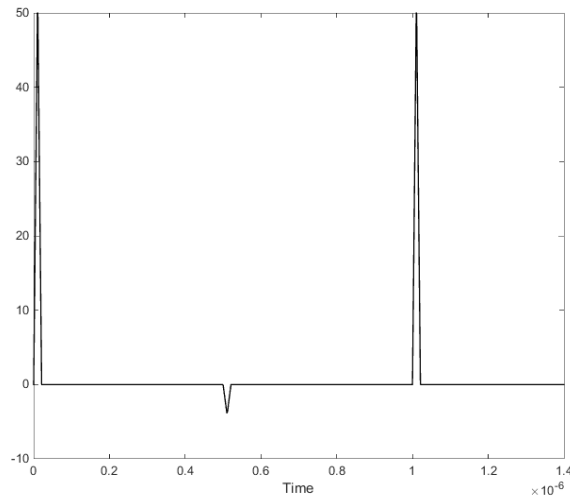

Fig. 4.8 Signal for intermediate fault (simulation result)

In Fig. 4.8 the discontinuity is located somewhere between the two ends of the cable. The round-trip time between two ends of the cable is 1 microsecond. The round-trip time between incident and reflected signals defines the fault location, and the reflection coefficient is a number between -1 and +1.

4.4 COMPONENTS OF MODIFICATION CIRCUIT

In order to investigate the feasibility of the proposed approach, the experimental setup should be prepared. The setup consists of a half bridge circuit, an injection circuit, and a pulse transformer.

4.4.1 HALF-BRIDGE CIRCUIT

A Half-Bridge DC-DC Converter is a type of DC-DC converter that can supply an output voltage either higher or lower than the input voltage. It consists of two switches, an upper and a lower switch [14]. The lower switch of a half bridge circuit can give a square wave form. The rise time of the square wave depends on the type of switches used.

Let us put the power converter application aside for a moment and focus on the square wave signal produced by the half bridge circuit and see if it is suitable for TDR purposes.

Below is a comparison between the square wave signals produced by an IGBT and a GaN device. Th Fig. 4.9 shows the drain-source voltage rise time of an IGBT device with its gate driver which are Microsemi-APTGF50X60T3G [15] and On Semiconductor-FAN3122TT [16] respectively.

28

X1= -17.8ns ΔX= 82.8 ns
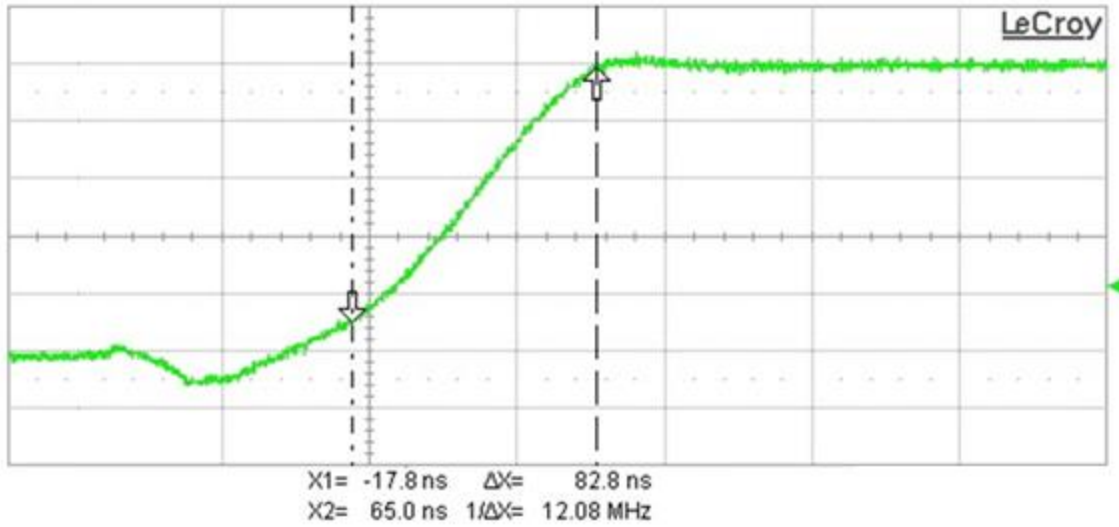X2= 65.0 ns 1/ΔX= 12.08 MHz

Fig. 4.9 IGBT drain-source voltage rise time

Similarly, the Fig. 4.10 shows the drain-source voltage rise time of a GaN MOSFET with its gate driver which are EPC-EPC2001[17] and TI-LM5113[18] respectively.
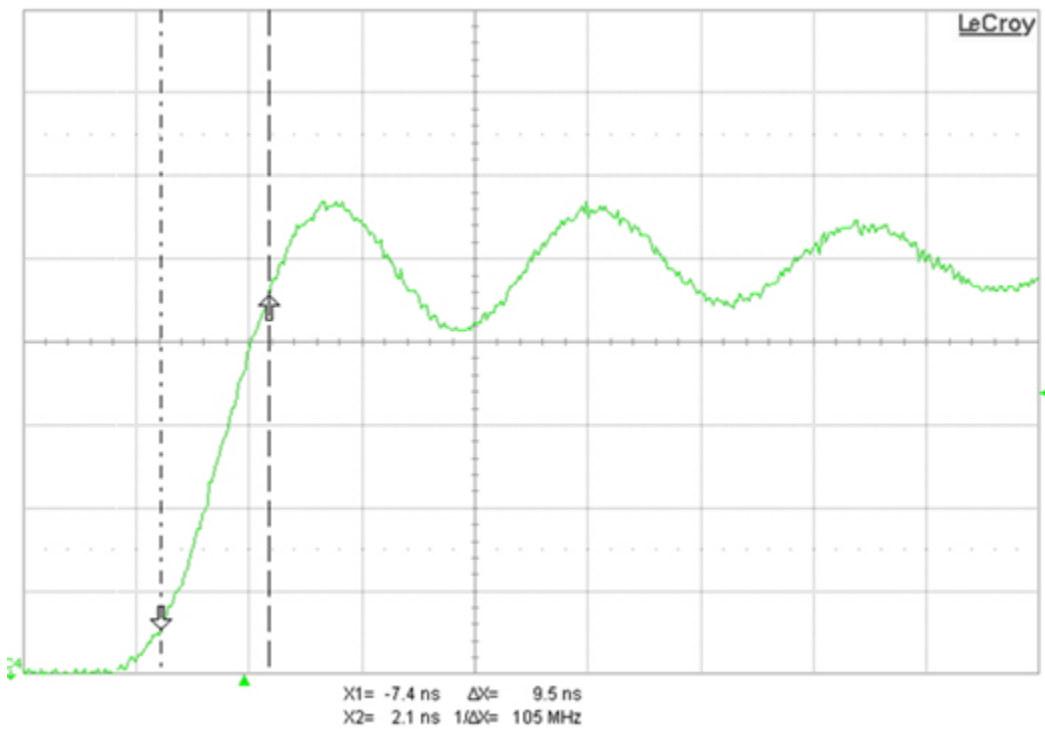

X1= -7.4 ns ΔX= 9.5 ns
X2= 2.1 ns 1/ΔX= 105 MHz

Fig. 4.10 GaN MOSFET drain-source voltage rise time

The switching time of the IGBT is about 80ns while it is 10ns for the GaN switch device. So, the GaN switch is clearly significantly faster. The faster rise time gives a much better spatial resolution. In Fig. 4.11, we use a square wave signal produced by a GaN switch device as an incident signal to detect the open and short terminations on a 10-meter cable. The velocity of propagation of an RG-58 coaxial cable is $2 \times 10^8 m/s$, so the round-trip time for a discontinuity at cable end is 100ns which matches with the experimental setup.
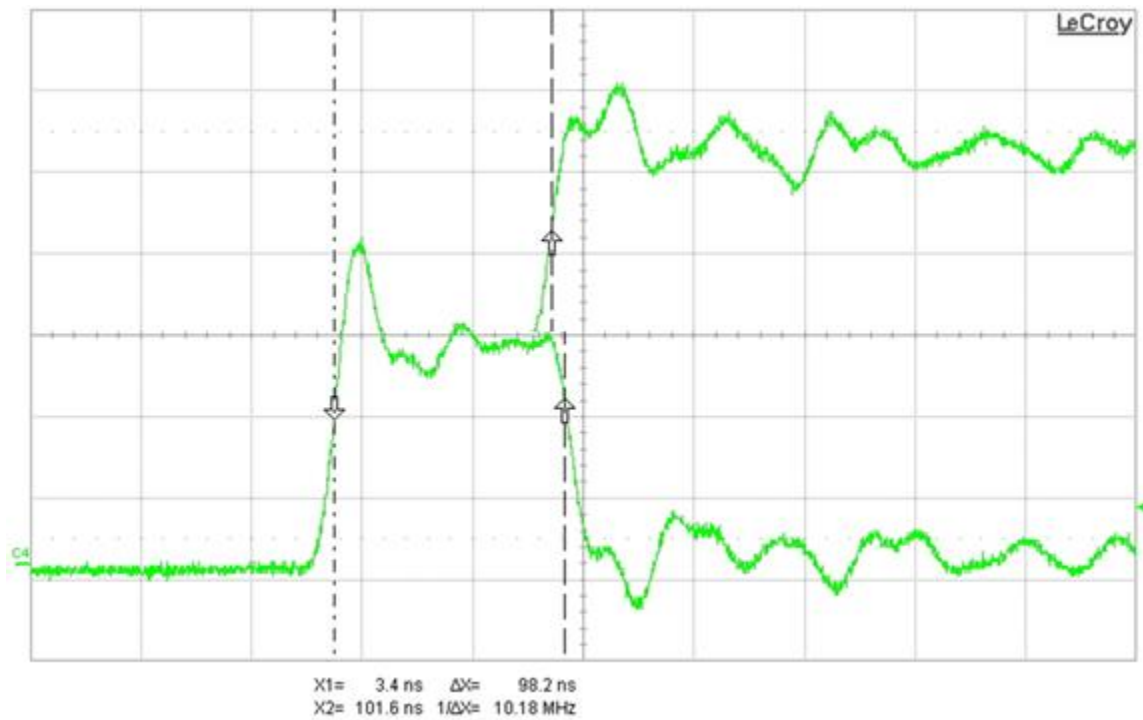

Fig. 4.11 TDR incident and reflected signal for open and short circuit cases

To summarize, GaN-based switches are fast enough to provide a good spatial resolution, so we are going to use a half bridge circuit with GaN switch implementation. The schematic diagram of the half bridge circuit is showed in Appendix A.

4.4.2 INJECTION CIRCUIT

The main function of the injection circuit is to empower an existing power converter to be a part of a monitoring system. As mentioned before, it is an RC circuit. In order to have a matched source and line, the value of R should be equal to the characteristic impedance of the cable i.e. 50Ω.

The capacitor determines the shape of the edge of the pulse: the smaller the capacitor value, the faster the rise time. The Fig. 4.12 shows incident signals corresponding to different capacitor values. Although the fastest incident waveform is desirable, it may cause resonance problem which can affect resolution. The origin of resonance is that the injection circuit is an RLC circuit and if the magnitude of capacitor and inductor are equal, the resonance occurs. So, instead of achieving the fastest rise time which may coincide with having resonance, the optimum fast rising time should be attained for each specific system. The initial value which is obtained by simulation was 3nF. We tried different capacitor values to find the smallest rising time and also the least resonance.
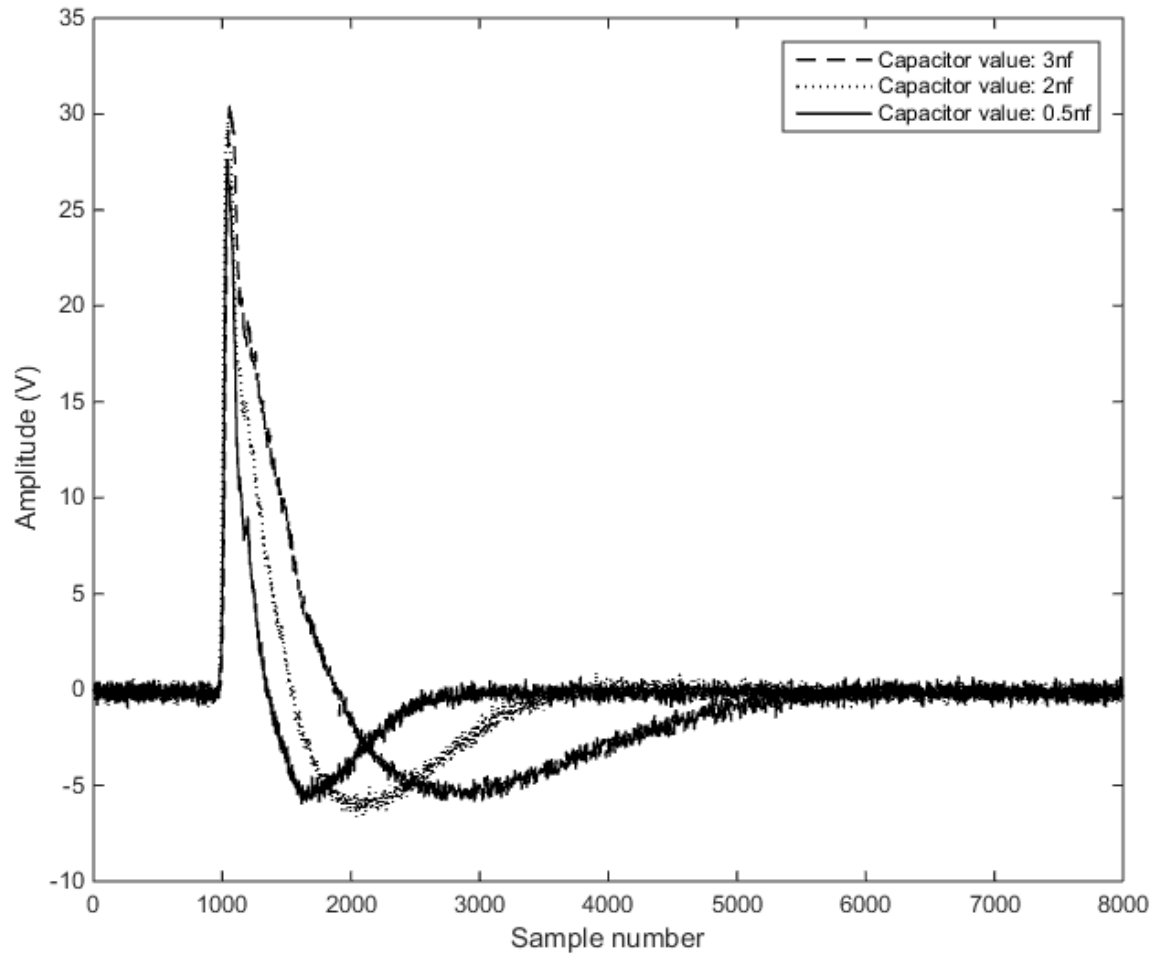
Fig. 4.12 Incident waveform for different capacitor values

As mentioned before, by decreasing the capacitor value, we can obtain an incident signal with faster rise time. Fig. 4.13 shows the effect of capacitor value on the TDR response of the cable.
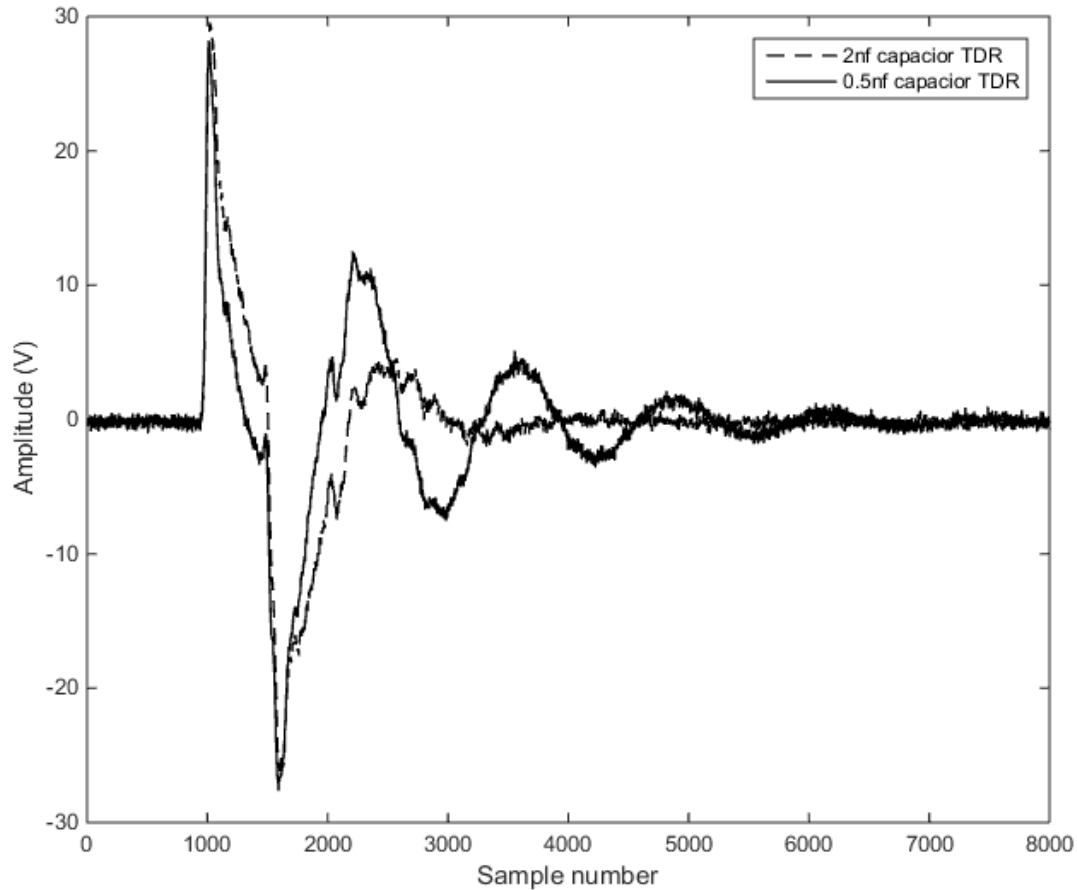
Fig.

4.13 TDR response based on capacitor value

The capacitor value of 2nF gives the best result, the fastest rise time, and the least resonance.

4.4.3 PULSE TRANSFORMER

The incident voltage is produced at the half bridge lower switch point; however, it should be transferred to the converter output. A pulse transformer is used for transmitting a fast rise signal when maintaining the fidelity of its shape is important. The pulse transformer is nothing more than a conventional transformer with a specific leakage and magnetizing inductance and a special magnetic core. Considering the pulse

33

transformer equivalent circuit and using MATLAB, Fig. 4.14 shows frequency response of a pulse transformer.
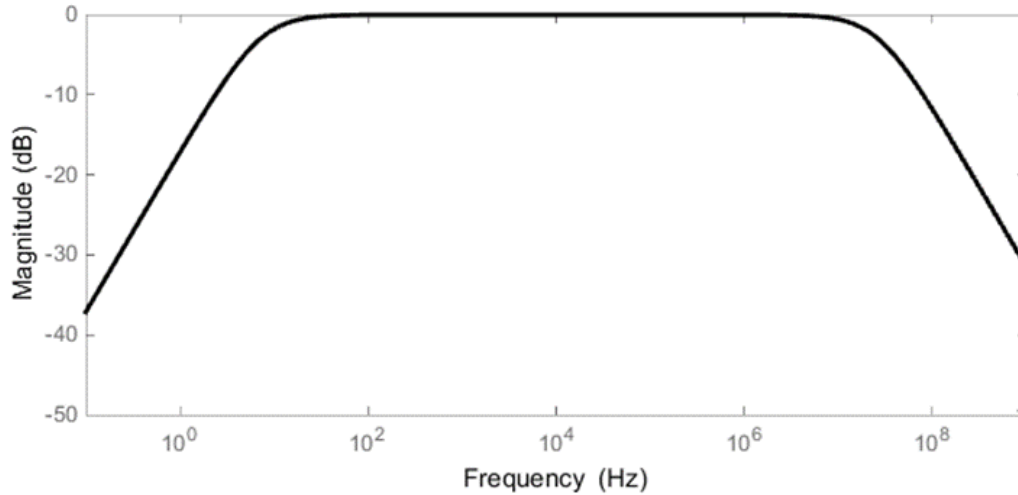

Fig. 4.14 Frequency response of a pulse transformer

The frequency response of desired pulse transformer and consequently its design parameters should be customized based on its input and the tracking performance that we have targeted.

The incident signal has a rise time of 10ns, In order to transfer the pulse with a minimum pulse distortion, especially during the rise time; a minimum bandwidth must be achieved [19].

$$BW_{GHz} = \frac{0.35}{RT_{nsec}} \quad or \quad RT_{nsec} = \frac{0.35}{BW_{GHz}} \qquad \begin{cases} RT: Rise\ Time \\ BW: Bandwidth \end{cases} \qquad (4\text{-}1)$$

$$BW_{GHz} = \frac{0.35}{10_{nsec}} = 35MHz$$

We need to choose a core material which can work in the desired frequency range. A perminvar NiZn ferrite is designed for high-frequency applications (up to 50

MHz) including pulse transformers, antennas and high frequency, high quality factor inductors.

In the next step, we need to focus on the frequency response of the pulse transformer to find the number of turns needed to achieve the required high bandwidth. There are no exact values for transformer inductances. We need to tradeoff between magnetizing and leakage inductances. Using simulation model in PLECS which is depicted in Fig. 4.15, we can play with the magnetizing inductance value until it gives the best result.
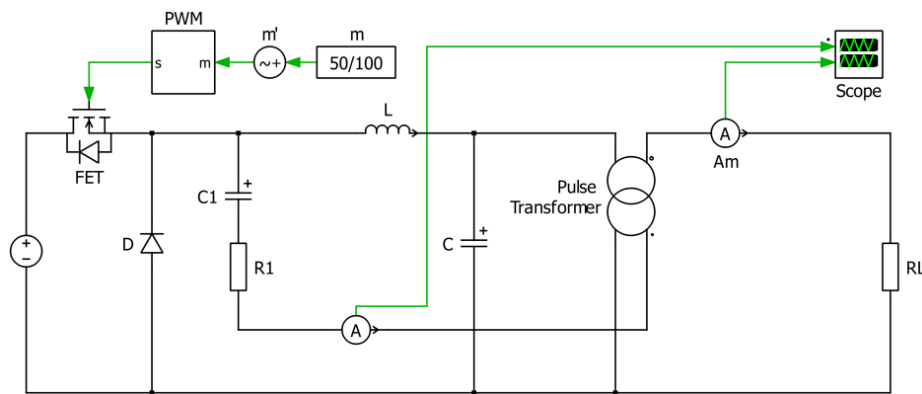

Fig. 4.15 Simulation model in PLECS

Knowing the desirable bandwidth and having the pulse transformer frequency response, the required leakage inductance can be found, so it is set to 100nH in the PLECS simulation. As it can be seen in Fig. 4.16, a pulse transformer with a large magnetizing inductance e.g. 1mH transfers the incident signal at its primary side to its secondary side without any changes.
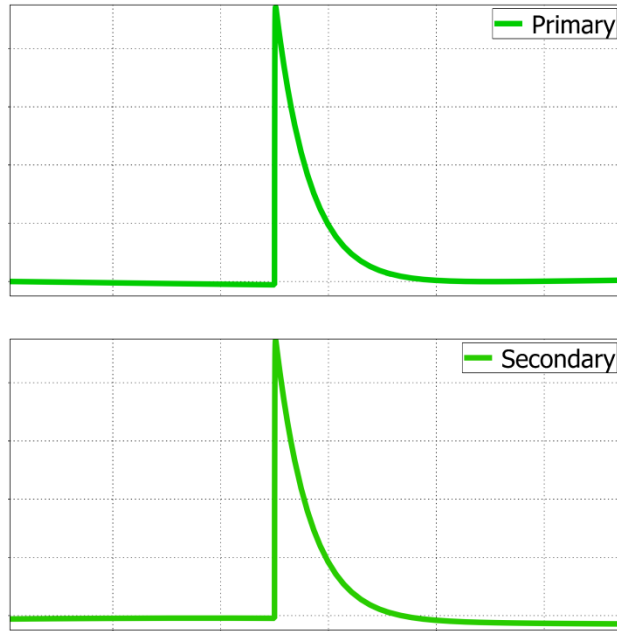
Fig. 4.16 Pulse transformer response with a large magnetizing inductance

We decrease the magnetizing inductance until the secondary side of the transformer still tracks its primary side properly (Fig. 4.17). The magnetizing inductance final value is 5µH.
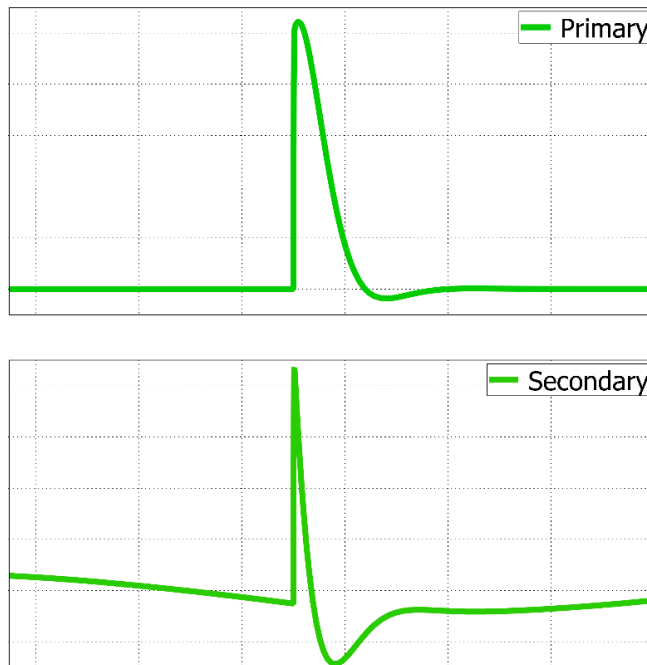

Fig. 4.17 Pulse transformer response with magnetizing inductance of 5µH

The transformer is designed based on the selected core shape and size and magnetizing inductance value we just determined. Characterizing the transformer is the next step after it has been built. It gives the real leakage and magnetizing inductances of the transformer. In order to characterize the pulse transformer, two sets of measurement need to be done. The measurements were taken by a 10Hz-500MHz network analyzer, Agilent 4395A. Magnetizing and leakage inductances are measured by open and short circuits test respectively [20]. Fig. 4.18 shows the impedance of the primary by shorting the secondary side. The leakage inductance is equal to primary inductance at the phase degree of 90. It is two times of each winding leakage inductance.

$$Leakage\ inductance = \frac{10^{\frac{12.69}{20}}}{2\pi \times 2 \times 4.263e6} = 80nH$$
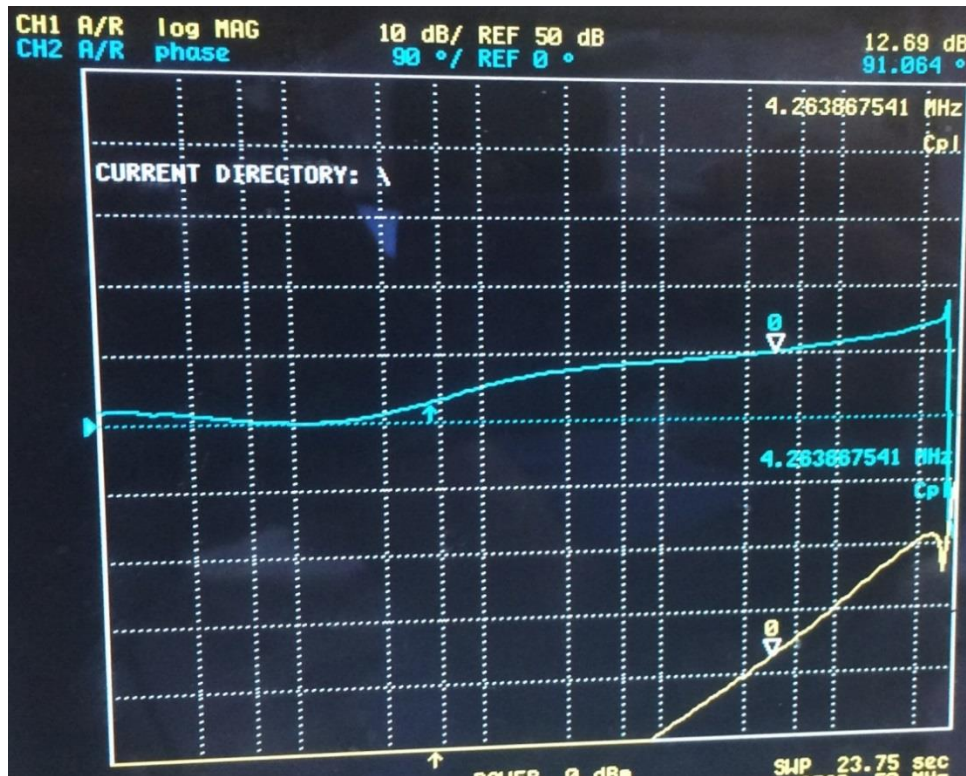

Fig. 4.18 Transformer primary inductance with short circuit at secondary side

Similarly, Fig. 4.19 shows the impedance of the primary by opening the secondary side. The magnetizing inductance is equal to primary inductance at the phase of 90 degree.

$$Magnetizing\ inductance = \frac{10^{\frac{21.34}{20}}}{2 \times \pi \times 344.8e3} = 5.3\mu H$$
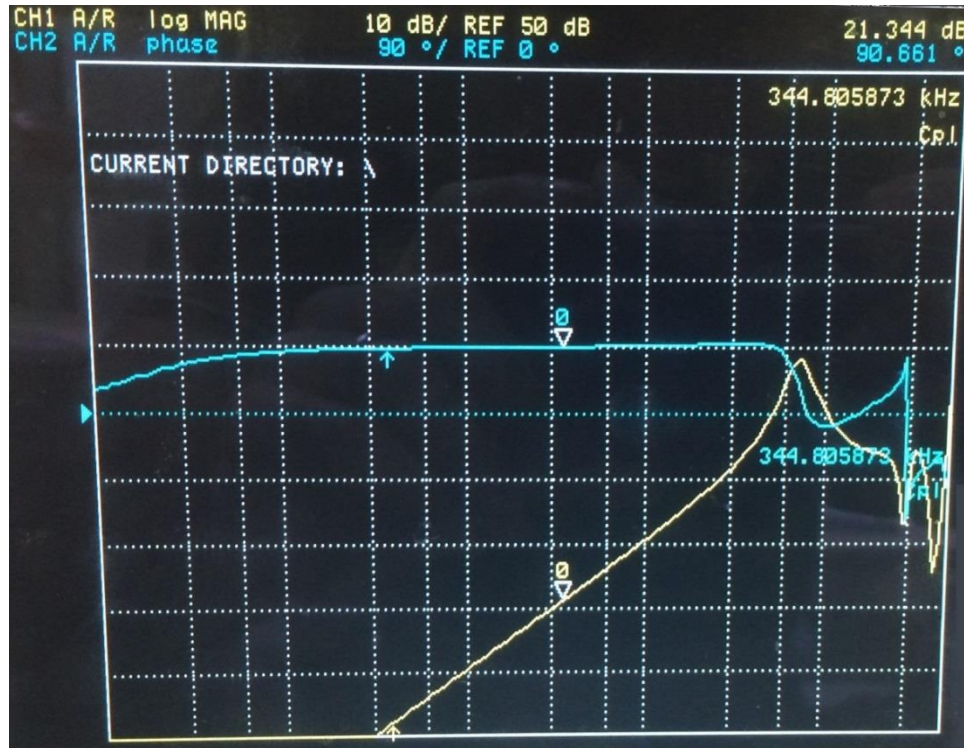

Fig. 4.19 Transformer primary inductance with open circuit at secondary side

Now, we have the pulse transformer inductances. Fig. 4.20 shows the pulse transformer frequency response.
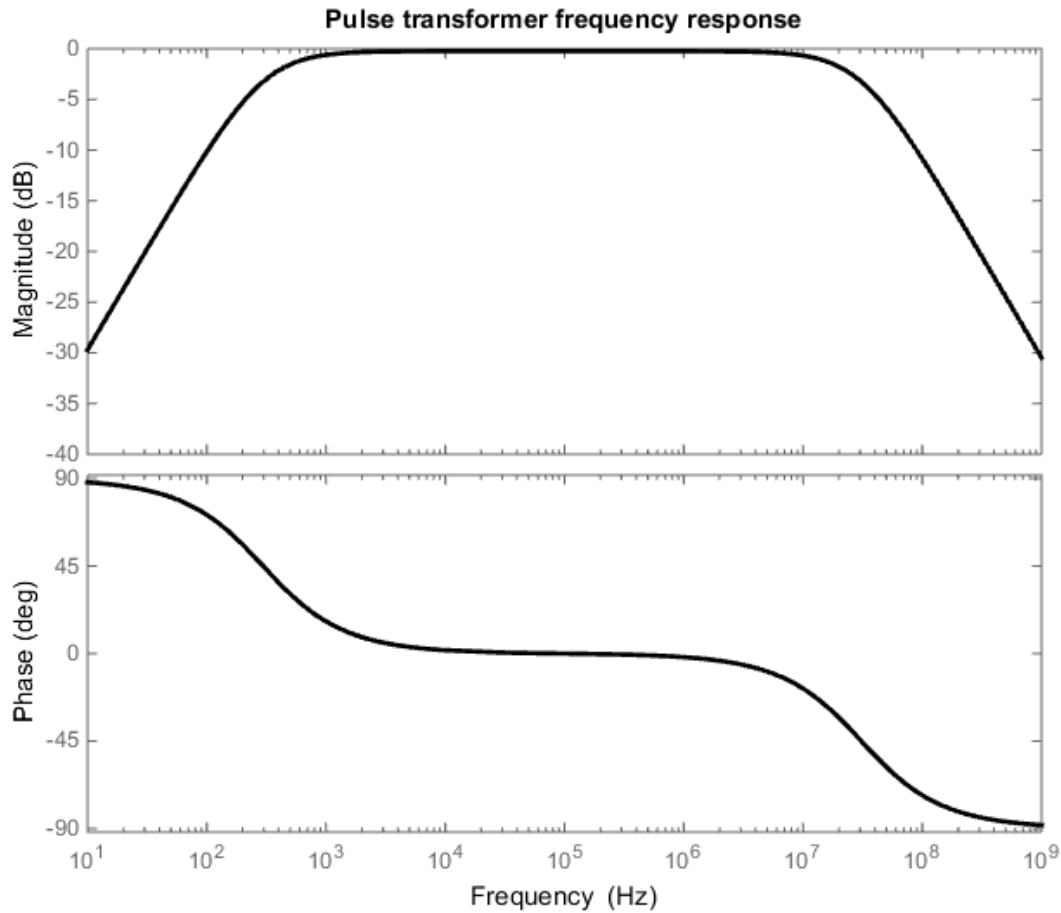
Fig. 4.20 The frequency response of the designed pulse transformer

In Appendix B, we describe the frequency behavior of the pulse transformer and go through transformer design procedure by obtaining the design parameters of the transformer we use for experimental setup. According to Appendix B, the transformer should be wound with 12 turns of 24 AWG.

Once the half bridge and injection circuit and pulse transformer are built, we can start the final experimental measurements.

CHAPTER 5

EXPERIMENTAL RESULTS

5.1 INTRODUCTION

As described in Chapter 4, the setup consists of a half bridge circuit, an injection circuit, and a pulse transformer. A picture of the experimental setup is shown in Fig. 5.1. Measurement were taken using a 10 GS/s digital oscilloscope.
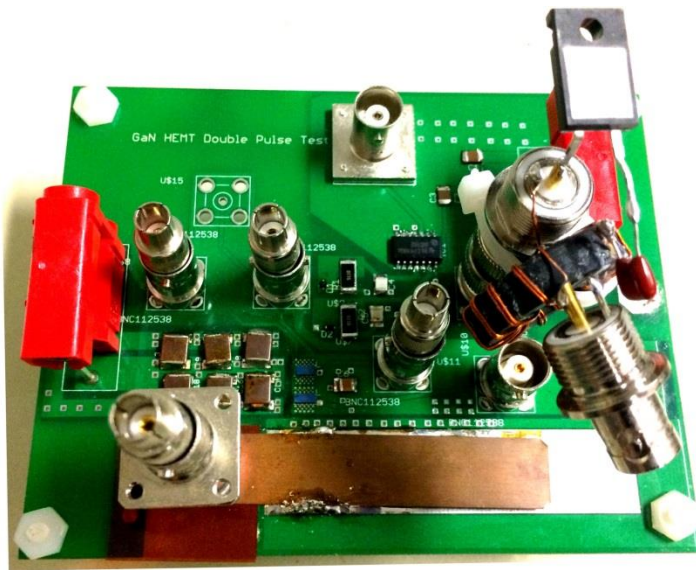

Fig. 5.1 Experimental setup

In Appendix A, we describe the design and operation of this circuit and provide the circuit schematic. Referring to Fig. 4.4, the RC circuit produces the incident waveform; this is transferred to the cable through the pulse transformer. In a real application, the configuration is a bit different. Here, we only send the incident signal along the cable while there is no DC power being transmitted, however in the real application, as shown

in Fig. 4.4, the incident signal is injected into the converter output. Notice that the converter output does not have any effect on the primary side of the pulse transformer since the converter load current is DC and it produces a constant flux in the pulse transformer, so no induced voltage is produced. The pulse transformer should be able to carry the converter current at its secondary without saturating.

This Chapter consists of two parts. In the first part, the experimental data is presented and in the second part signal processing is performed on this data to calculate the fault distance and type.

5.2. ACQUIRING EXPERIMENTAL DATA

There are two main kinds of cable faults: hard faults and soft faults. The hard faults are open or short circuits, which lead to a large change in cable characteristics at the fault location. This causes a large incident signal reflection, which is relatively easy to detect. Conversely, soft faults are caused by discontinuities of the impedance in the cable, for example due to damaged insulation. In this case the reflection is smaller in amplitude and can be difficult to detect.

5.2.1 HARD FAULTS

As mentioned above, hard faults are open or short circuit faults. Two sets of measurement are made for each case to investigate the method capability for different lengths of the cable.

Before considering the hard faults, it is a good idea to get familiar with the actual incident waveform which is used in the measurement. The incident waveform has a fast-

rising time and a relatively long-lasting trailing end region which is indicated in Fig. 5.2. The trailing end region is caused by magnetizing inductance of the pulse transformer. As magnetizing inductance increases, the trailing end region decreases. A larger magnetizing inductance, obtained using a larger number of turns in the pulse transformer, also causes a larger leakage inductance, which decreases the pulse transformer bandwidth, as explained in Appendix B. The design choice is to select a smaller magnetizing inductance, trading off a longer trailing end region for a larger pulse transformer bandwidth, which gives a steeper rising edge and therefore better space resolution.
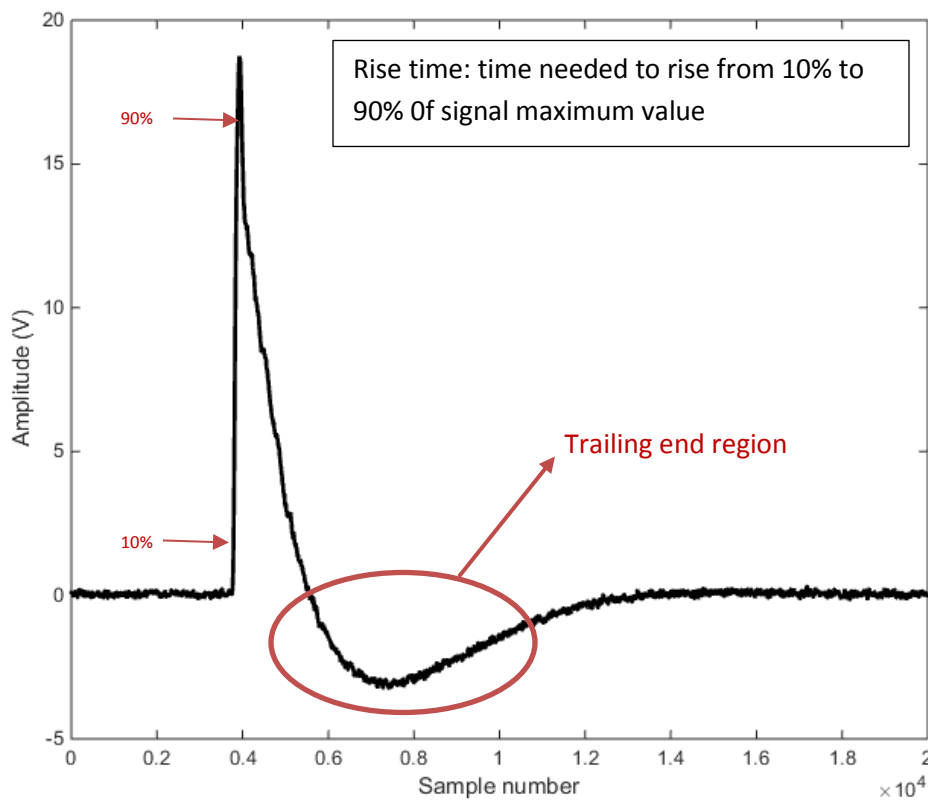

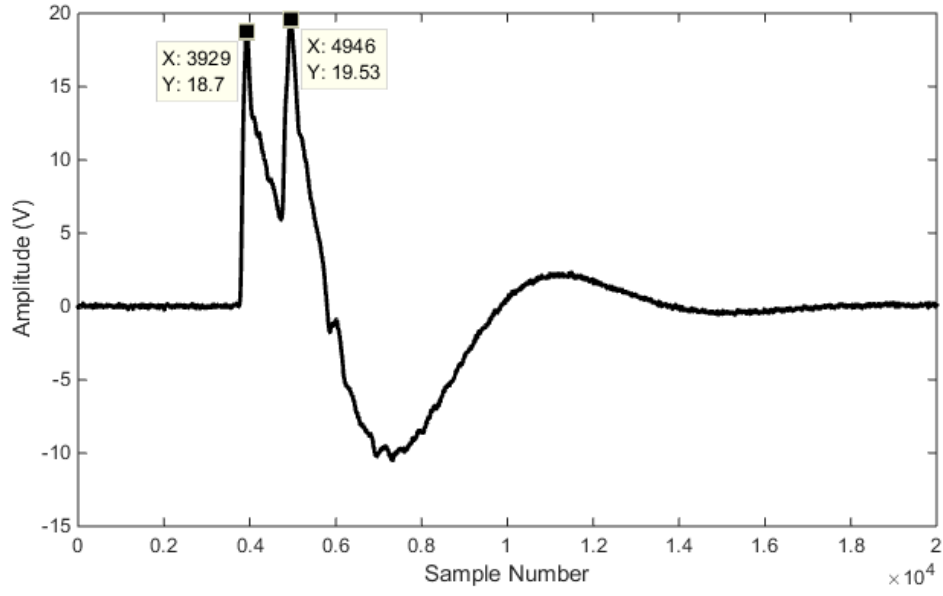Fig. 5.2 Incident signal used for measurement

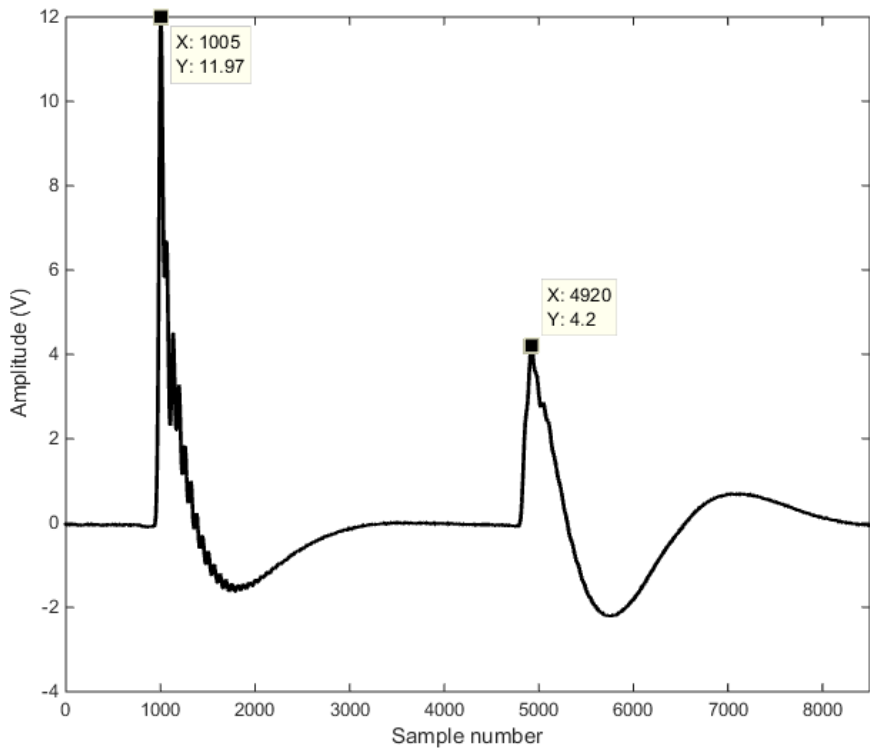Fig. 5.3 Open circuit case, incident and reflected signal, 10-meter cable

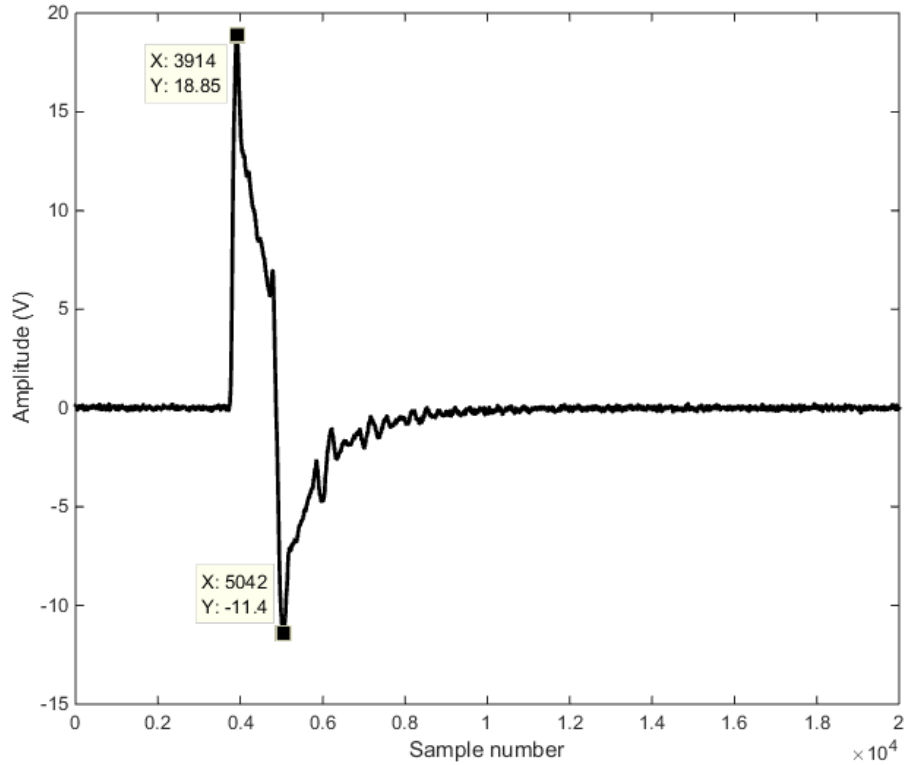Fig. 5.4 Open circuit case, incident and reflected signal, 80-meter cable

Fig. 5.5 Short circuit case, incident and reflected signal, 10-meter cable

Fig. 5.3 and 5.4 show the incident and reflected signal for two cable lengths, 10m and 80m, respectively. Comparing Fig. 5.3 and Fig. 5.4, the reflected signal overlaps with the incident signal in the 10-meter cable. This effect causes some deterioration in the spatial resolution for faults located near the source. We address this issue in detail later.

5.2.2 SOFT FAULTS

Soft faults are caused by small variations in characteristic impedance of the cable. Unlike hard faults which interrupt the normal operation of the cable, they do not interrupt energy transmission but cause a long-term deterioration of the cable which can result in hard faults. The soft faults have different causes such as sheath damage, conductor

degradation, and insulation deterioration. They usually have a very small effect on TDR curve, so it is very challenging to detect them.

In order to verify the feasibility of the proposed approach for detecting soft faults, several experiments are conducted.

5.2.2.1 INSULATION DETERIORATION

Since even the best insulation does not provide perfect insulation, there is always a leakage current between a phase conductor and ground. As insulation deteriorates with age, the leakage current increases, so monitoring the leakage current is a tool for assessing the insulation health level. The leakage current can be modeled by a parallel resistor between the phase conductor and ground. We simulate the parallel fault to model insulation deterioration.
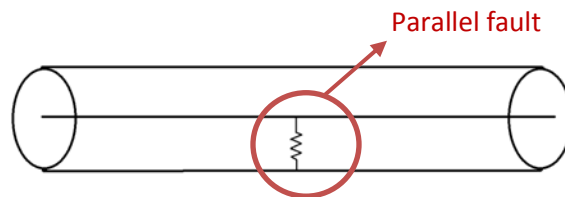

Fig. 5.6 Insulation deterioration model

In the model of Fig. 5.6, different resistor values represent different levels of insulation deterioration. In theory, for a healthy cable case, the resistor value is infinity, but in the real world, even a healthy cable has a small amount of leakage current in the order of microamperes, which is equivalent to a resistor value in the order of mega ohms in the insulation deterioration model.
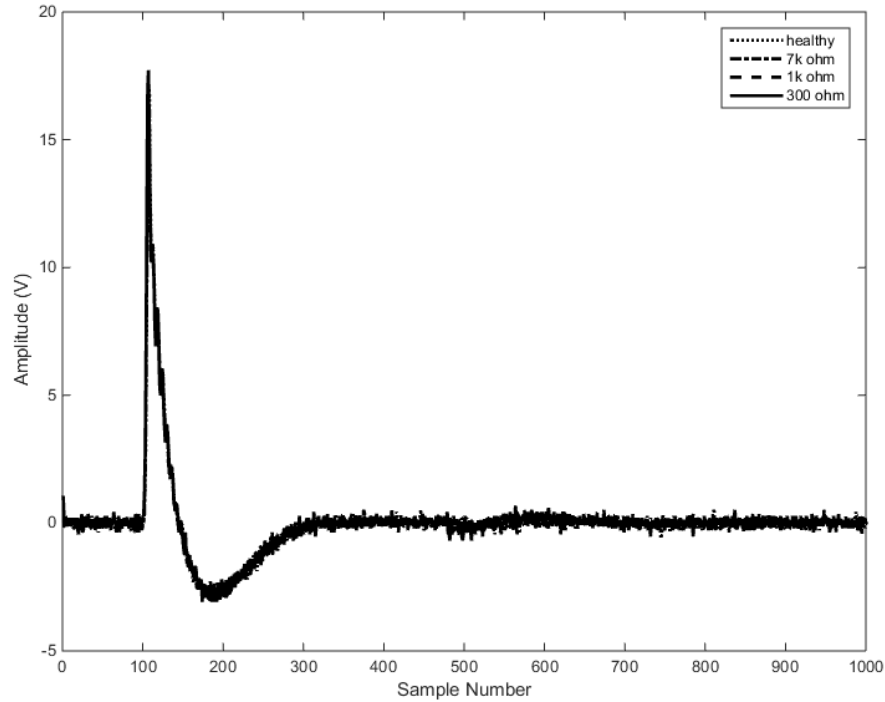
Fig. 5.7 Incident and reflected signal in the time domain for different levels of insulation

deterioration

Unlike hard faults, Fig. 5.7 shows that the time domain TDR waveform for soft faults is very similar to the healthy cable case. Therefore, signal processing is necessary to extract the cable fault information.

5.3. SIGNAL PROCESSING

In the experiment the incident signal is injected into the cable, travels down the cable with propagation velocity v_p and is reflected when it encounters the impedance discontinuity. A high-speed oscilloscope captures both incident and reflected waveforms.

We need to process the reflected signal in order to extract the effect of the discontinuity. For this purpose, cross-correlation tool is a good candidate. Cross-

correlation computes the correlation between the incident and reflected signal and measures how similar they are.

Cross-correlation is very similar to convolution. To calculate the convolution of two signals, one of the signals is mirrored about the y-axis and it is shifted by a certain amount. A third signal is obtained by multiplying element-wise these two signals. . By summing all values of the third signal, we obtain the convolution for that specific shift. Cross-correlation can be calculated in the same way except that mirroring is not applied to the signal.

Suppose we have x(n) and y(n) as sequence signals, the cross-correlation is:

$$r_{xy}(l) = \sum_{n=-\infty}^{+\infty} x(n)y(n-l) \tag{5-1}$$

$$r_{xy}(l) = \sum_{n=-\infty}^{+\infty} x(n+l)y(n) \tag{5-2}$$

The index l is the shift or lag. It provides a measure of how much the two signals are similar based on a specific shift in time.

Cross-correlation of a signal with itself is called auto-correlation. Obviously, the autocorrelation of a signal is maximum at l=0.

$$r_{xx}(l) = \sum_{n=-\infty}^{+\infty} x(n+l)x(n) \tag{5-3}$$

If the signals which are cross-correlated are scaled, while the shape of cross-correlation does not change, the amplitude changes due to the scaling.

To compensate for the scaling effect, the normalized cross-correlation should be used. The normalized auto and cross correlation are defined as: [21]

$$\rho_{xx} = \frac{r_{xx}(l)}{r_{xx}(0)} \tag{5-4}$$

47

$$\rho_{xy} = \frac{r_{xy}(l)}{\sqrt{r_{xx}(0)r_{yy}(0)}} \qquad (5\text{-}5)$$

Considering the open and short circuit case, the reflection coefficients are 1 and -1 respectively. So, there is a positive/negative maximum of cross correlation between the incident and reflected signal at a lag equal to the round-trip time for open/short circuit cases. The maximum normalized cross correlation value is 1.

Two considerations are of order; first, in the real world, the reflected signal amplitude is smaller than the incident signal due to attenuation and dispersion and filtering behavior of the cable. Second, it is hard to extract the incident and reflected signal off the measuring signal which includes both incident and reflected signals at least in case of an extremely soft fault condition.

In Fig. 5.3 the discontinuity location is near the source, so the reflected signal overlaps with the incident signal. The incident signal is independent of the cable condition and we characterized that before, so by subtracting the incident signal from the acquired signal, the reflected waveform can be obtained.

Having separated the incident and reflected signal, we can calculate the cross correlation between them to find out how much they are similar and what is the characteristic and location of the fault.

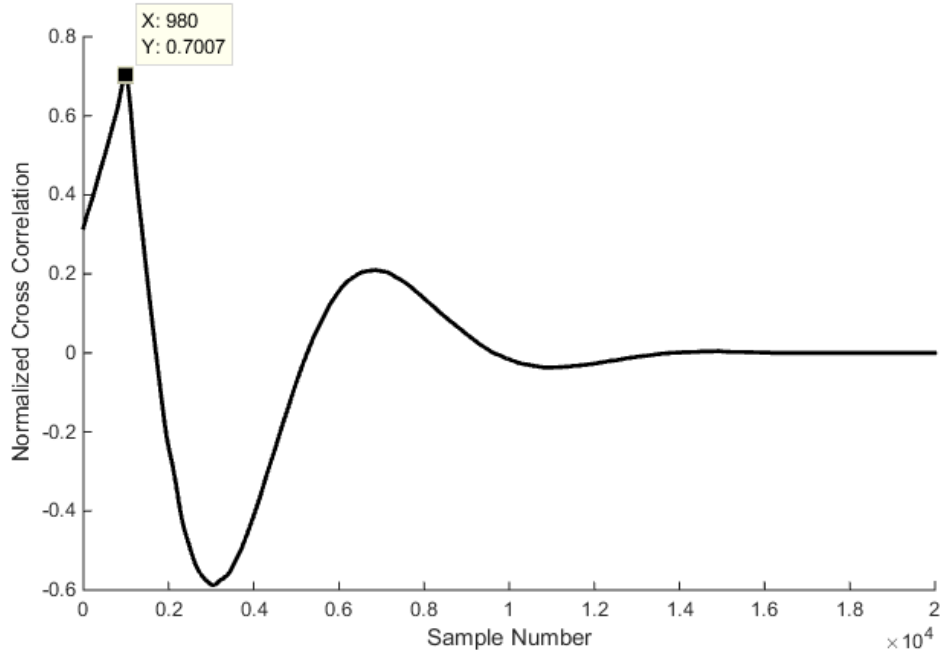At first, we consider hard faults in the 10-meter cable.

Fig. 5.8 Normalized cross correlation between the incident and reflected signal

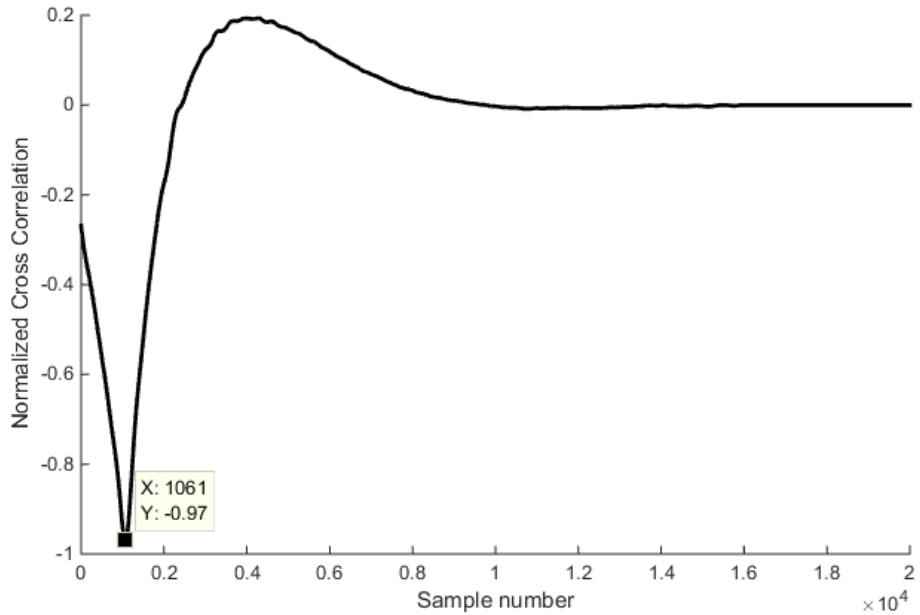10-meter cable, open circuit at the end

Fig. 5.9 Normalized cross correlation between the incident and reflected signal

10-meter cable, shorted at the end

Analyzing the cross-correlation results, the hard faults are detectable and locatable. The first peak (with either positive or negative sign) provides some information regarding the fault. Theoretically, we expect a normalized cross correlation of 1 for open circuit and -1 for short circuit, but, as mentioned before, due to attenuation and dispersion and filtering behavior of the cable, the cross-correlation value gets smaller.

Fig. 5.8 shows the case of an open-ended cable. The sample number associated with the first cross correlation peak gives the location of the fault which is 980. The sampling period is 0.1nS, so the fault location would be 9.8 meters away from the source. Using Fig. 5.3, the correct value should be 1020 or equivalently 10.2 meters away from the source. This means that the process of separating the incident and reflected signal and the signal processing performed cause an error of 4% in this case.

Likewise, for shorted cable, comparing Fig. 5.9 and Fig. 5.4 gives an error of 5%.

Sample number can be related to the time using the scope sampling period. The time difference gives the round-trip time which can be translated to the fault location if the propagation velocity is known, as described before.

The next case we consider is the 80-meter open ended cable. At first, the incident and reflected signals are extracted from the acquired signal. Fig. 5.10 shows the cross correlation between the incident and reflected signal. Same as before, the sample number associated with the first cross correlation peak gives the location of the fault which is 3910. The sampling period is 0.2nS, so the fault location would be 78.2 meters away from the source. Using Fig. 5.4, the correct value should be 3915 or equivalently 78.3 meters away from the source
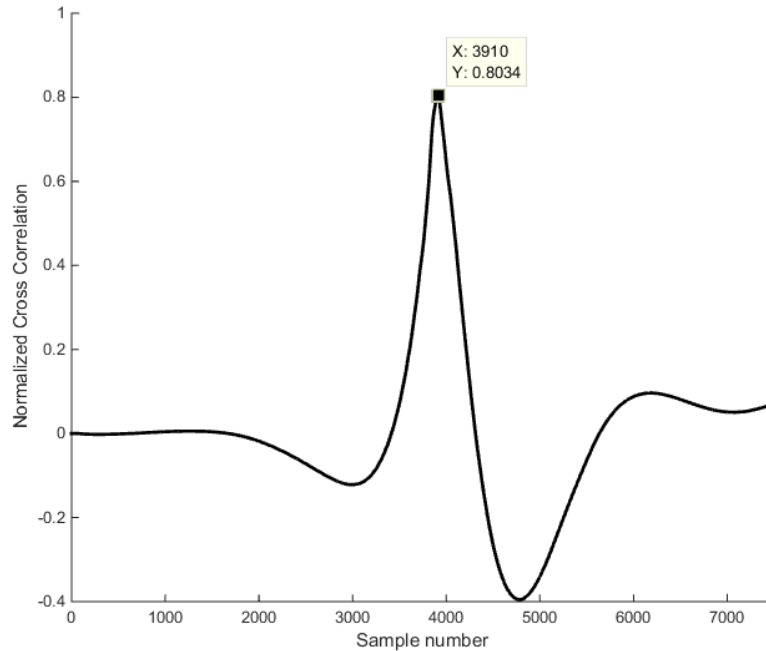
Fig. 5.10 Normalized cross correlation between the incident and reflected signal,

open ended, 80-meter cable

In comparison to the 10-meter cable case, the error is much smaller, less than 1%. The reason is that the incident and reflected signals are separated in time and they do not interfere with each other. If the fault is located near to the source, the method faces some problems in locating the fault. That is why the distance between rise and trailing end of the incident signal is called dead zone; faults in this area are not located accurately. Some commercial time domain reflectometers use an attachment lead longer than the width of the incident signal to deal with this issue [22]. It moves the fault to a location beyond the dead zone. By adding the attachment lead, it takes more time for incident signal to encounter a discontinuity and return to the source again, so incident and reflected signals do not overlap anymore.

51

Considering soft faults, the fault detection is more challenging and extracting the incident and reflected waveform from the acquired signal is not as easy as before, so a different approach will be taken.

Considering the matched load, the acquired signal gives the incident signal alone because there is no reflection. This is the *baseline* for the healthy case. In case of fault, the acquired waveform consists of both the incident and reflected signals. If we calculate the cross correlation between the waveforms of these two cases, we will have two peaks, one at the time zero which is caused by incident signal and another at a time equal to round trip time which is caused by reflected signal. Obviously, we are interested in the second one.

The signal acquired from matched loaded cable is considered as the baseline record. The autocorrelation of the baseline is considered as signature of the healthy cable.

For cases other than healthy cable, the acquired signal consists of the incident and reflected signals, even if the reflected signal may not be detectable in the time domain waveform. This signal is cross correlated with the baseline. By comparing the autocorrelation and cross correlation results, the condition of the cable can be investigated. Any deviation from the healthy condition indicates a fault.

In the insulation deterioration model, the largest parallel resistor that is detectable using this approach is 7kΩ which is equal to a reflection coefficient of -0.03. The leakage current would be 14mA in a 100-volt system.
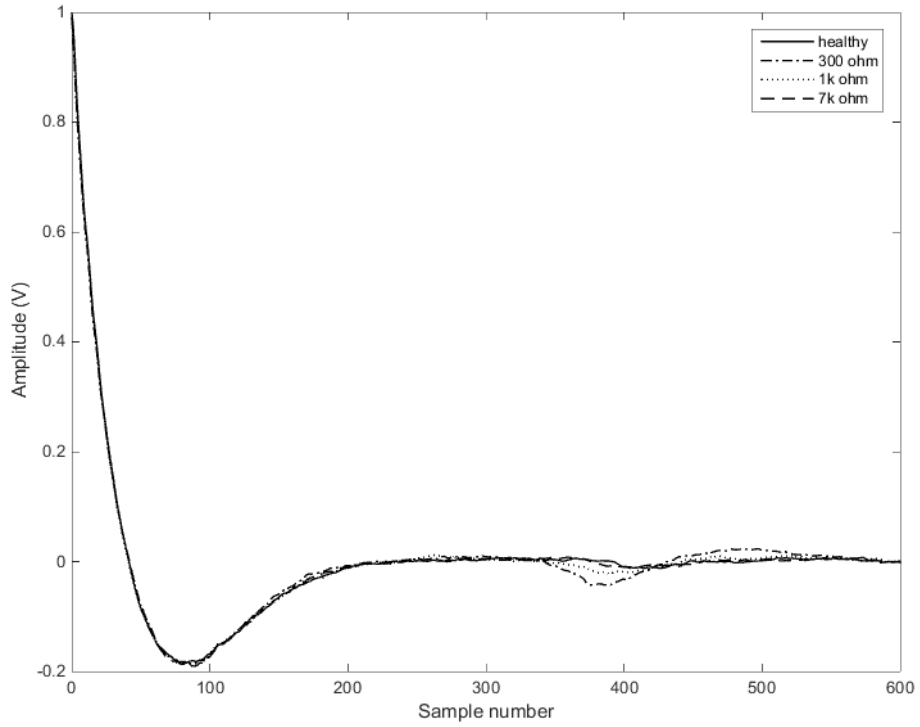
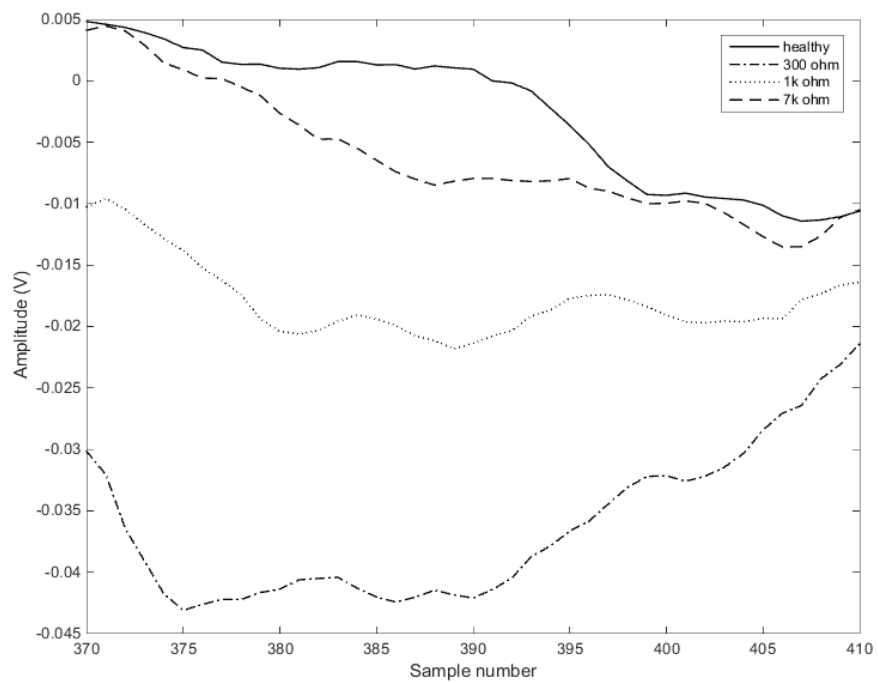Fig. 5.11 Normalized cross correlation, comparing the baseline and faulty cable

Fig 5.12 Zooming in at deviation area of Fig. 5.11

Theoretically, even a very small soft fault should be detectable using this approach or other signal processing methods. For example, in [23] the statistical cross correlation is used, which is a powerful tool and more sensitive in comparison to conventional cross correlation. We applied that method on the acquired signals, however because of noise level, it does not provide good results in compare to conventional method. What is the origin of measurement noise? The problem comes when we try to detect an extreme soft fault that causes a tiny reflected signal, so there is a small signal in the presence of a relatively large signal. We acquire signals using an oscilloscope. Digital oscilloscopes include a high-speed analog to digital converter which has 8-bit resolution. It means that there are 256 distinct voltage levels to full scale. In this case, we have a small reflected signal in the presence of a large incident signal, so the LSB becomes relatively large and can become larger than reflected signal amplitude. So, inherent sampling noise of scope can overwhelm the reflected signal [24]. Different oscilloscopes have different tools to decrease the measuring noise such as averaging and high-resolution acquiring which are addressed in [25]. We already used these tools when we are acquiring the signals.

In order to detect soft faults that have subtle effects on reflection waveforms, it is necessary to deal with and reduce measurement noise.

CHAPTER 6

CONCLUSION

The following conclusions can be drawn from the investigation.

The feasibility of proposed embedded cable health monitoring system within power converter has verified by several experiments.

Time domain reflectometry method is able to detect and locate different types of fault, including hard faults and soft faults.

An existing power converter can be modified so that it can be used for time domain reflectometry to monitor the condition of the cable which is connected to it.

Several experiments have been conducted in this project to verify the feasibility of this approach. As a result of this investigation, it has been shown that GaN based switches are fast enough to provide good spatial resolution for fault detection for the cases considered.

The signal produced by injection circuit can be used for TDR purposes and experimental results have shown the feasibility of the proposed setup.

Overlapping the incident and reflected signal can reduce the accuracy of fault locating. The measurements show that this method has the smallest error for the faults with separately incident and reflected signals. The incident and reflected signals would be separate if the round-trip time was greater than incident pulse width which means faults located at least 50 meters away from the source.

The method works well with relatively large reflections which reduce the effect of noise. In order to detect soft faults that have subtle effects on reflection waveforms, it is necessary to deal with and reduce measurement noise.

This method can be used for cable age estimation as a future work. A new cable has a well-known propagation velocity. Since the propagation velocity is inversely proportional to the square root of the dielectric constant which decreases as cable gets older, the aging of the cable can be tracked by measuring how the propagation velocity changes over time. Several works [26], [27] have done to simulate accelerated aging. The same method can be used to do aging simulation for a specific cable and find out the relation between the propagation velocity and its aging level.

REFERENCES

[1] R. Mobley," An introduction to predictive maintenance", second edition, Elsevier Science, USA, 2002

[2] K. O'Connor, C. Dowding, "Real time monitoring of infrastructure using TDR technology", GeoTDR Inc.

[3] S. Mukhopadhyay," New developments in sensing technology for structural health monitoring", Springer, New Zealand, 2011

[4] B. Celaya, "DSL line tester using wideband frequency domain reflectometry," Master Thesis, University of Saskatchewan, Canada, August 2004

[5] C. Sharma, C. Furse, "Low-Power STDR CMOS Sensor for Locating Faults in Aging Aircraft Wiring", IEEE sensors journal, Vol. 7, No. 1, January 2007

[6] J. Wang, P. Stone, D. Coats, Y. shin, R. Dougal, "Health monitoring of power cable via joint time-frequency domain reflectometry", IEEE transactions on instrumentation and measurement, Vol. 60, No. 3, March 2011

[7] D. Coats, "Comprehensive joint time-frequency analysis toward condition based maintenance regimes for electrical and mechanical components", PhD dissertation, University of South Carolina, USA, 2014

[8] Y. Shin, C. Hong, E. Song, J. Yook, "Application of Time-Frequency Domain Reflectometry for Detection and Localization of a Fault on a Coaxial Cable", IEEE transactions on instrumentation and measurement, Vol. 54, No. 6, December 2005

[9] J. Strickland, "time-domain reflectometry measurements", Tektronix

[10] Time Domain Reflectometry Theory, Application Note, Agilent technologies

[11] David M. Pozar, "Microwave Engineering", 4th edition, Wiley, 2012

[12] R. Erickson, D. Maksimovic, "Fundamentals of power electronics", Second edition, University of Colorado, Springer, 2007

[13] A. Rusek, S. Ganesan, B. Oakley, D. Aloi, "Time-Domain Reflectometry (TDR) in graduate courses,, Oakland University, School of Engineering and Computer Science

[14] Half-Bridge DC/DC Converters Electronics, Power Supply Technology, Mouser Electronics

[15] IGBT Modules Power Module, Microsemi, Data sheet manual

[16] Single 9A, high speed, low side gate driver, On Semiconductor, data sheet manual

[17] Enhancement Mode Power Transistor, GaN switch, EPC2001, EPC, data sheet manual

[18] Half-Bridge Gate Driver for Enhancement Mode GaN FETs, LM5113, TI, data sheet manual

[19] Understanding oscilloscope bandwidth, rise time and signal fidelity, Technical brief, Tektronix

[20] Agilent Impedance Measurement Handbook, A guide to measurement technology and techniques, 4th Edition, Agilent technologies

[21] J. Proakis, D. Manolakis, "Digital Signal Processing", 3rd edition, Prentice-Hall International Inc. USA, 1996

[22] The fastest, most accurate method of locating faults in metallic cables, SONEL Test and Measurement Instruments (http://www.sonel.pl)

[23] G. Cerri, R. De Leo, L. Della Nebbia, S. Pennesi, V. Primiani and P. Russo, "Fault location on shielded cables: Electromagnetic modelling and improved measurement data processing", IEE Proc.-Sci. Meas. Technol., Vol. 152, No. 5, September 2005

[24] Evaluating High-Resolution Oscilloscopes, Application Note, Agilent technologies

[25] Michael Lauterbach, "Making More Accurate Measurements Using Digital Oscilloscopes", LeCroy, Application Brief, November, 2011

[26] L. Hore, O.Chavez, "Thermal aging effects on coaxial cable 's transmission and its life expectancy", International wire & cable symposium proceeding, 1998

[27] Assessing and managing cable aging in nuclear power plants, International Atomic Energy Agency, Vienna, 2012

[28] V. Spataro, "Design high performance pulse transformers in easy stage", GEC Marconi Electronic Systems Corp - March, 1995

[29] National Magnetics Group website, Materials & shape tables

[30] Toroid Application Notes, Ferronics Inc

APPENDIX A – HALF-BRIDGE CIRCUIT

The half-bridge configuration is one of the most common switch circuit topologies used in power electronics applications such as synchronous buck converters and voltage source converter.

The half-bridge circuit consists of an upper and lower switch. As discussed in Chapter 4, in order to have sufficient spatial resolution, we select a Gallium Nitride based switch which has a fast switching time.
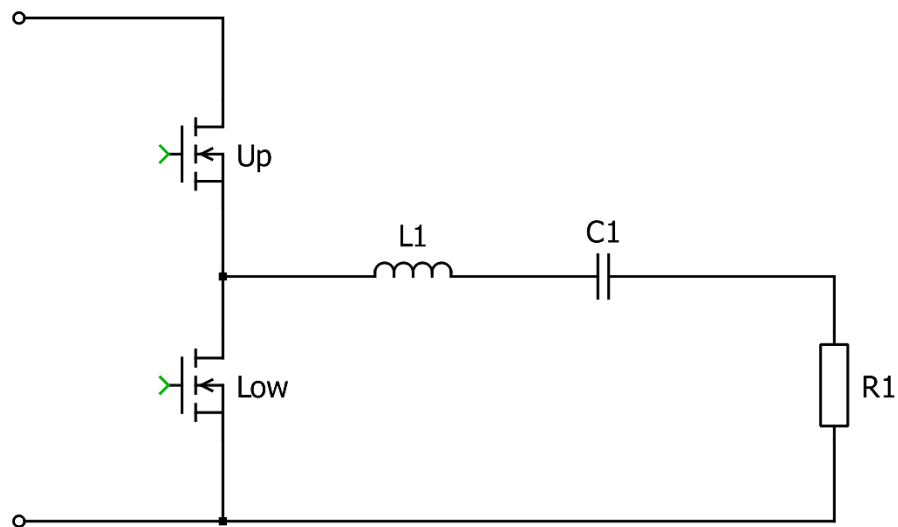

Fig. A.1 Half bridge circuit and RLC load

The circuit includes a DC voltage bus input, a midpoint i.e. the common point between the upper and lower switch, a ground return and the gate drivers for switches (Fig. A.1)

The switches are turned on and off in a complementary fashion by a Half-Bridge Gate Driver (TI, LM5113) as it is showed in Fig. A.2. It drives both the high and low side enhancement mode GaN MOSFET in a synchronous buck or a half-bridge circuit.
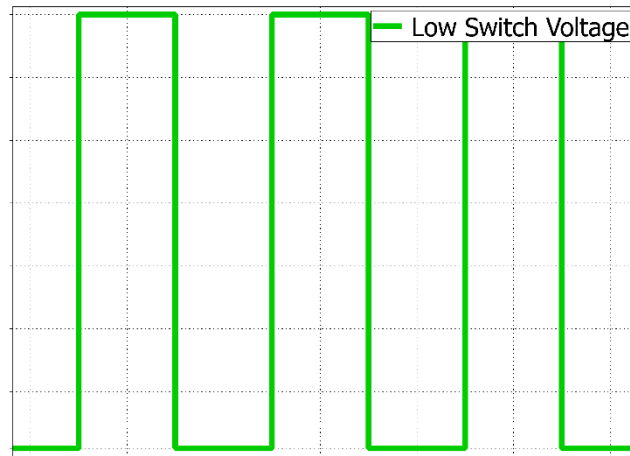

Fig. A.2 The low switch voltage waveform

We are using a previously designed GaN HEMT double pulse tester designed by Dr. K. Peng (previous member of the PEG at USC) in this thesis.

The Fig. A.3 shows the gate driver circuit for high-side and low-side switches. It consists of three main components:

1. Quad 2-Input NOR Gate (ON Semiconducor, MC74AC02)
2. Low Quiescent Current LDO Regulator (Microchip, MCP1703)
3. Half-bridge gate driver for Enhancement Mode GaN FETs

The purpose of the NOR Gate is to generate high-side and low-side driver control inputs for gate driver with a small dead time to prevent shoot-through. The 5 V supply of the circuit is provided by the MCP1703 LDO regulator. The outputs of half-bridge gate driver go to the gates of the GaN-based switches.

The Fig. A.4 shows the power diagram. The input voltage is hooked up to the connector on the right side of the layout. There are two switches which are driven by the gate driver described above.

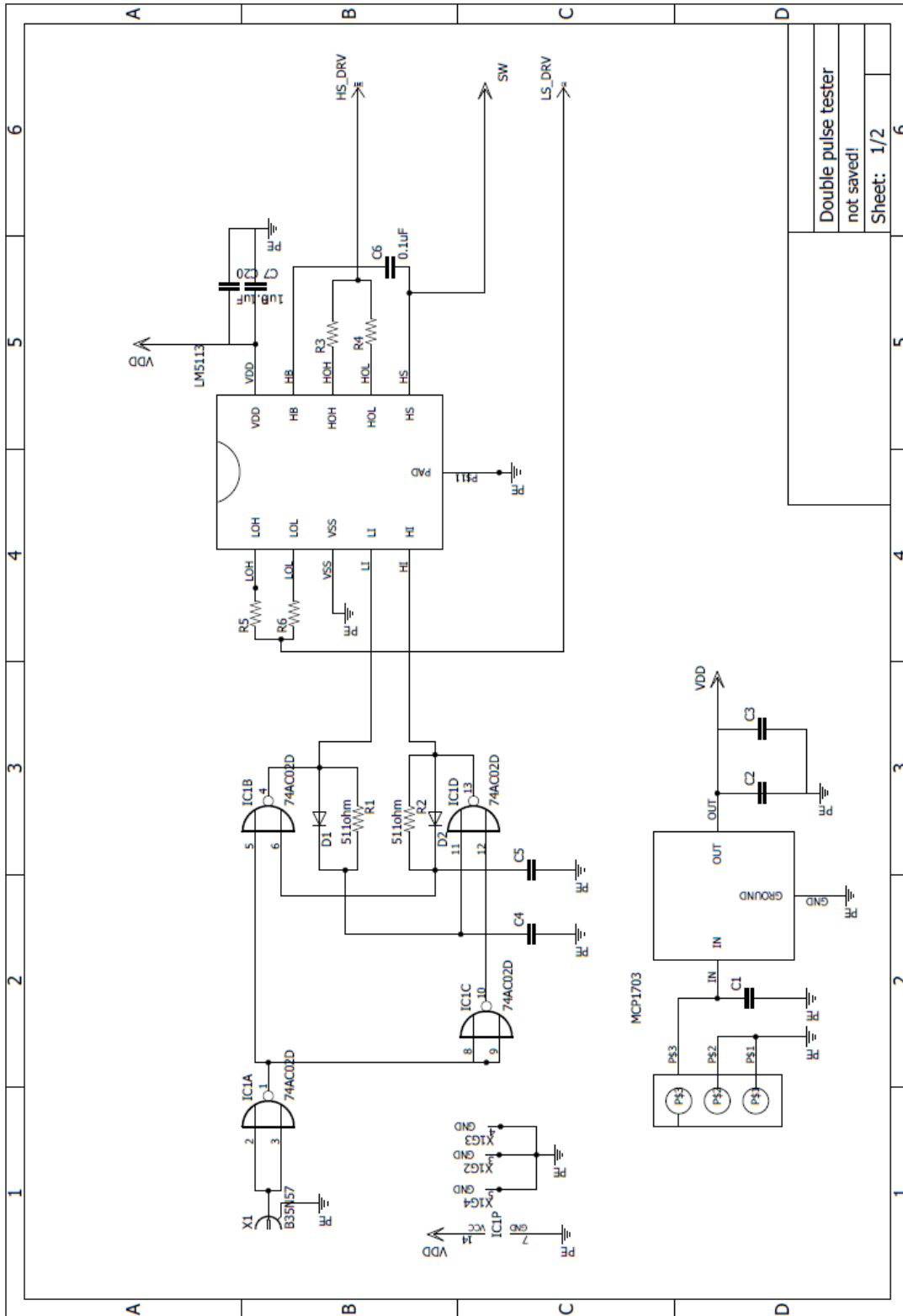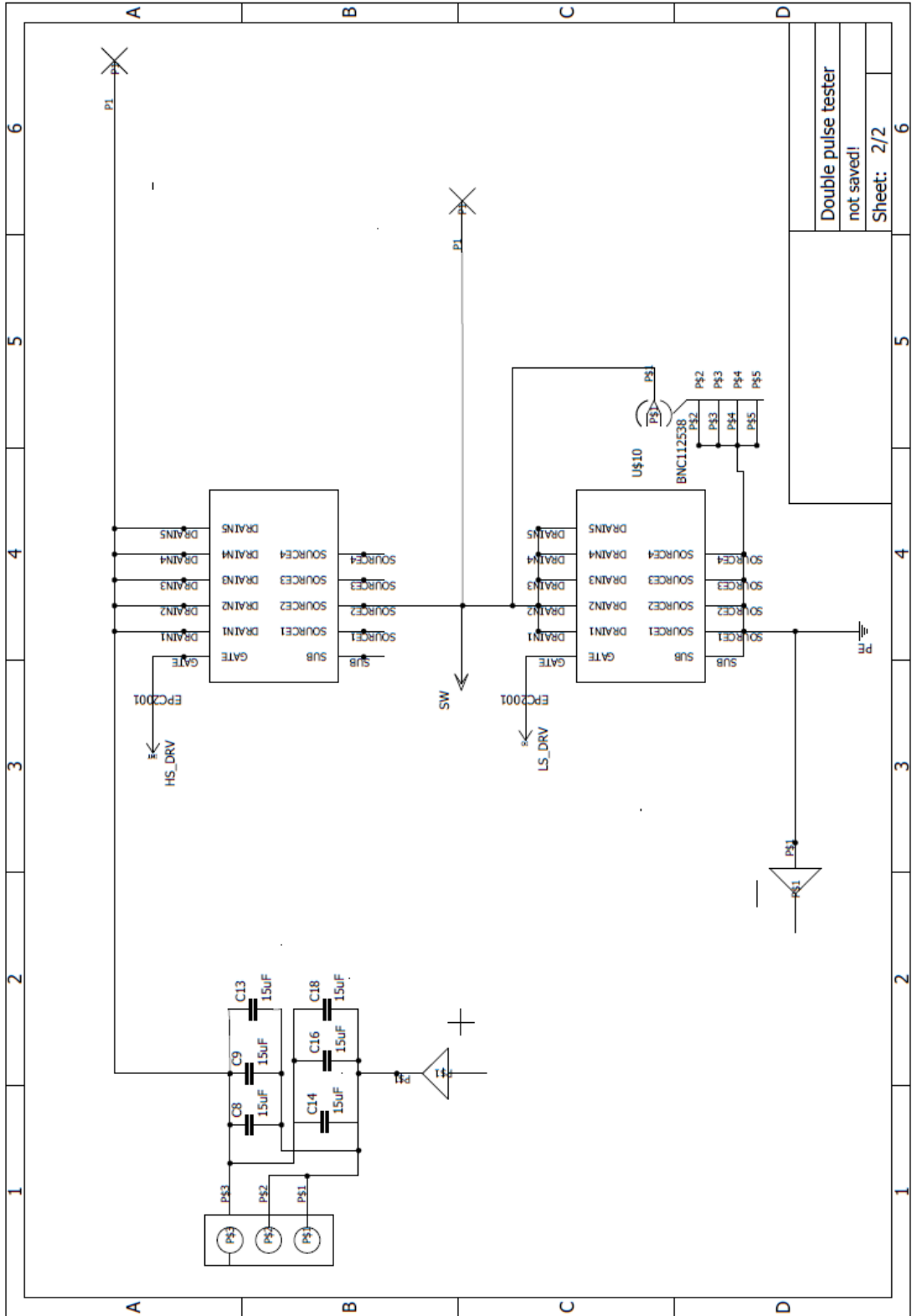The input of the injection circuit is connected to the half-bridge midpoint.

Fig. A.3 Gate driver circuit for high-side and low-side switches

Fig. A.4 Half-bridge power diagram

APPENDIX B – PULSE TRANSFORMER DESIGN

A Pulse transformer transfers a current or voltage pulse with minimum distortion in the signal shape from the primary side of the transformer to the secondary side. The equivalent circuit of a pulse transformer has been shown in Fig. B.1. The signal applied to the primary side of a pulse transformer may have different shapes, such as rectangular, trapezoidal or even a spike. Design criteria is different for each shape in some sense, however the principle is the same.
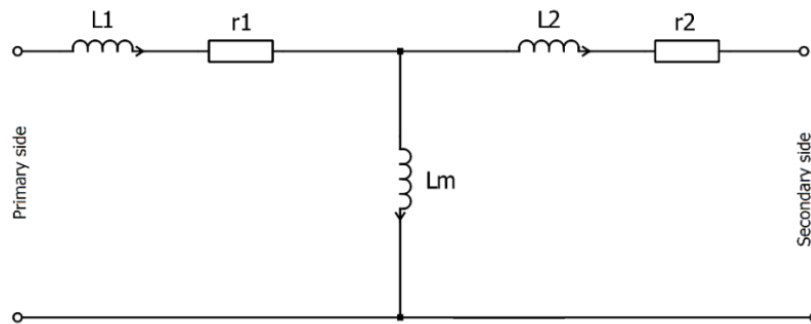

Fig. B.1 Equivalent circuit of a pulse transformer

To get familiar with frequency behavior of a pulse transformer, we select a rectangular signal.

An ideal rectangular signal has a zero rising and falling time. In the real world, the voltage cannot change instantaneously so there is a finite rise and fall time. (Fig. B.2)
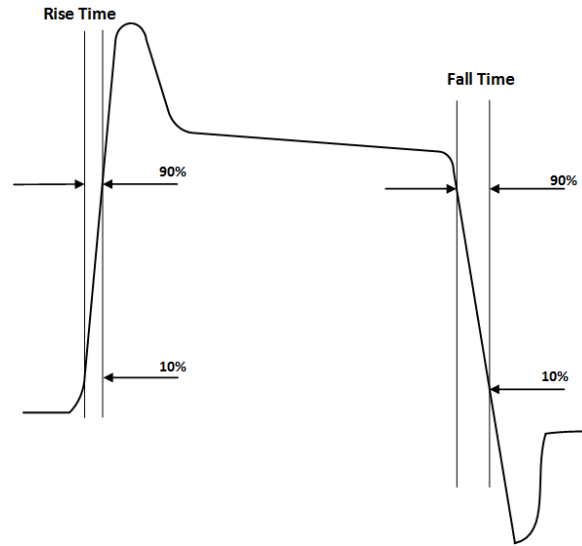
Fig. B.2 A real pulse waveform

Besides having the rising and falling region (high frequency region), there is a flat region (low frequency region) which is the main part of signal and its length depends on signal duty cycle [28].

Considering the low frequency region, the leakage inductance can be neglected. So, the circuit is simplified to diagram of Fig. B.3.
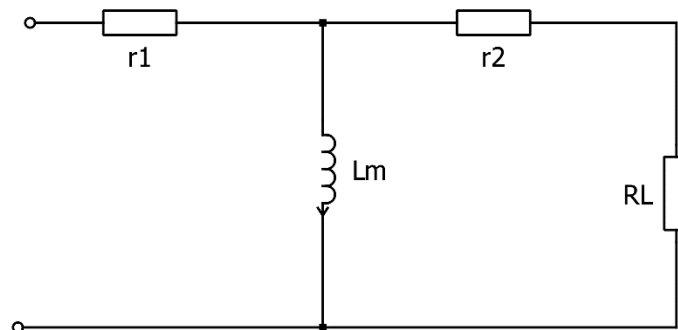

Fig. B.3 Low frequency equivalent circuit diagram

Obviously, it is a high pass filter, so the pulse transformer attenuates low frequency signals, i.e., it has a lower bandwidth. The cross-over frequency is $f_c = \frac{R}{2\pi L_m}$. Fig. B.4 shows the simplified low frequency circuit of pulse transformer and it bode plot.
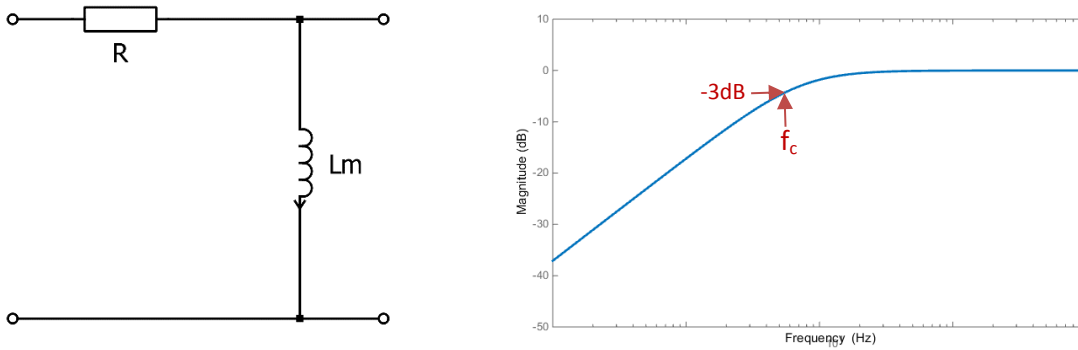

Fig. B.4 A high pas RL filter with a cross-over frequency at f_c

As frequency increases, magnetizing reactance increases until $\omega L_m \gg R_L$. Now we can neglect the magnetizing inductance too. So the pulse transformer equivalent circuit changes to Fig. B.5. In this region, we have a frequency-independent gain; the gain is limited by winding resistances.
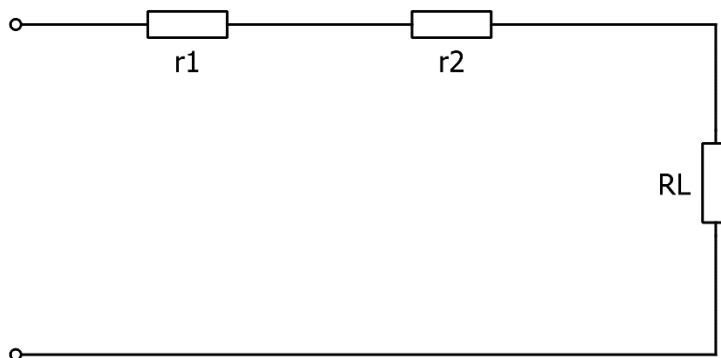

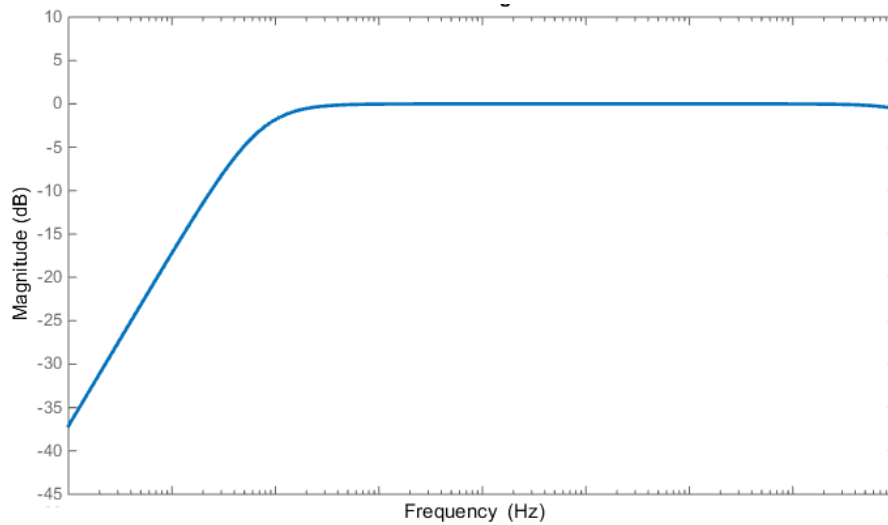Fig. B.5 Middle frequency range equivalent circuit

Fig. B.6 Middle frequency response of pulse transformer

The leakage inductance value is small and is in the order of nH. Therefore, we could neglect it at low frequencies. However, at higher frequencies, the leakage reactance is not negligible anymore and must be considered at higher frequencies. Also, the magnetizing inductance can be neglected because of its high impedance at high frequencies. The equivalent circuit at higher frequencies is shown in Fig. B.7.
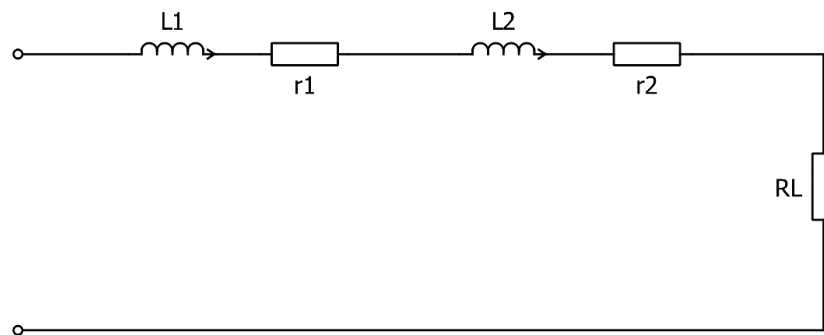

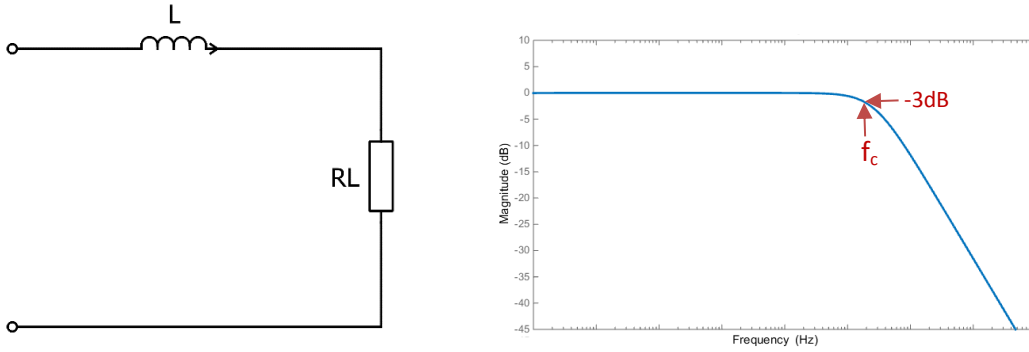Fig. B.7 High frequency equivalent circuit diagram

Fig. B.8 A low pas RL filter with a cross over frequency at fc

In conclusion, we can say that the frequency response of a pulse transformer depends on its magnetizing and leakage inductance. The magnetizing inductance defines the low frequency behavior and the leakage inductance defines the high frequency behavior.

The incident signal we are using is a pulse signal. So, it mostly has high frequency components. So, having a leakage inductance as small as possible is the first design priority. Large magnetizing inductance is desired but it leads to a higher leakage inductance. So, the goal is optimizing the magnetizing inductance and minimizing the leakage inductance.

Our goal is to transfer the incident signal to the converter output. The rise time of the incident signal is 10ns so the its bandwidth is $BW_{GHz} = \frac{0.35}{10_{nsec}} = 35MHz$.

Based on bandwidth of the signal, the core is selected. The selected core should be able to work in the desired frequency range. The core material is Ferrite: NiZn.

property	initial perm-eability	satur-ation flux density	loss factor [@frequency]	curie temp.	volume resistivity	recommended freq.	common shapes
unit		gauss	10^{-6}	°C	Ω^{-cm}	MHz	
M2	40	2300	<150[50MHz]	450	10^7	0.1-50	toroid, rod, balun

Table B.1 The core material specifications [29]

In this step, the core geometry is chosen. A Ferrite toroid provides a convenient and effective shape for winding the pulse transformers. The winding must fit through the window. It is necessary to define the core dimensions. We picked the core with ID=0.5 inch, OD=1 inch, H=0.25 inch.

	outside diameter		inside diameter		thickness			core constant	effective path length	effective cross sectional area
Toroids							mass	$\Sigma l/A$	le	Ae
p/n	in.	(mm)	in.	(mm)	in.	(mm)	grams	cm^{-1}	cm	cm^2
1015-1	1.000	25.40	0.500	12.70	0.250	6.35	12	14.3	5.5	0.39

Table B.2 The toroid core geometry [29]

In a toroidal core, the magnetizing inductance is [30]

$$L = 2\mu N^2 2.5H \ln\frac{OD}{ID} \times 10^{-9} Henries \qquad (B\text{-}1)$$

If the formula is rewritten for the number of turns,

$$N = 2218.391 \sqrt{\frac{L}{H.\ln\frac{OD}{ID}}} \qquad (B\text{-}2)$$

By using simulation model and trial and error, the L is defined as 5 µH. Knowing the inner and outer diameter and core thickness, N=12 turns.

We use the same number of turns for both primary and secondary windings, so $\alpha = 0.5$. The fill factor K_u is the fraction of the core window area which is occupied by copper. It should be selected between zero and one, so we take 0.5.

The cross-sectional area of the conductor, A_w is expressed as

$$A_w \leq \frac{K_u \alpha W_a}{N} \qquad \text{(B-3)}$$

where W_a is core window area.

From the above inequality, $A_w=0.026\text{cm}^2$ is an acceptable value, which corresponds to a 14 AWG wire.

Since we defined the secondary current of pulse transformer 1 Amp, we can reduce the wire size; it gives not only a smaller leakage inductance, but convenience in winding process. Finally, we have a pulse transformer with specifications as Table B.3.

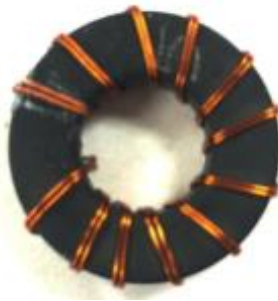| Pulse transformer spec			
Core shape	toroid	Magnetizing inductance	5μH
Core material	Ferrite	Leakage inductance	80nH
Number of turns	12		

Table B.3 Pulse transformer specifications

Fig. B.9 Designed pulse transformer

A photo of built pulse transformer can be seen in Fig. B.9.